Faculty of Mathematics and Computer Science
Heidelberg University

Bachelor Thesis in Mathematics
submitted by

Antonia Seifert

2022

CAT(0) geometry, Gromov's link condition and its applications to discrete settings

This Bachelor Thesis has been carried out by Antonia Seifert at the
Mathematical Institute
of Heidelberg University
under the supervision of
JProf. Dr. Beatrice Pozzetti

Abstract

A powerful tool to generalize the concept of curvature to metric spaces is the comparison of triangles in them to those in model spaces. This notion of curvature, known as CAT(κ) geometry, can be applied to different metric spaces. In this thesis, I concentrate on cube complexes on the one hand and give a simplified proof of Gromov's link condition, which relates the CAT(0) property to a combinatorical one. On the other hand, I transfer the CAT(0) geometry concepts to discrete settings and investigate its relation to defects in quivers. In this way, I show the existence of connections between the lack of positive vertex defect in quivers, chart defects and the CAT(0) property. In particular, a square lattice with defects fulfills the discrete CAT(0) inequality if and only if it does not harbour any positive vertex defects. Furthermore, I prove that the presence of chart defects is equivalent to the chart complex violating the CAT(0) property. Through these chart complexes, I find a link from quiver geometry to CAT(0) cube complexes. This connection can be used for further research through the application of the tools of CAT(0) cube complexes and their links to discrete setting.

Contents

1 Introduction and overview

An important concept within the geometry of manifolds is the curvature. There are several different but related concepts of curvature, such as the sectional curvature and the Riemann curvature tensor. More generally, curvature of general metric spaces can be studied as well. This can be done by comparing geodesic triangles, as introduced by A. D. Alexandrov in 1951 [Ale51; BH99]. By comparing the distance of points on the circumference of a triangle in the metric space and in a model space, the so-called CAT(κ) spaces can be studied where κ is a real number. Since this was done by Cartan, Alexandrov and Topogonov, among others, their names are considered in the terminology. The number κ denotes the curvature of the model space used for the comparison. In the case of manifolds, the curvature in the CAT(κ) sense can be related to the sectional curvature. However, it can be defined for general metric spaces and for cube complexes. In the latter case, being CAT(0) can be related to the link complex of the vertices being flag by the so-called *Gromov's link condition*.

In this thesis, I will introduce and discuss the general case of CAT(0) geometry as well as its characterizations and the connection to the sectional curvature in the case of manifolds (Section 2). For cube complexes, I will prove Gromov's link condition in Section 5 in a simpler way than given in [BH99]. Furthermore, these concepts can be applied to discrete settings, as in the case of quivers described in Section 3. It can then be related to defects in the quivers (Sections 3 and 4) and the chart complex of the quiver defined in Section 6.

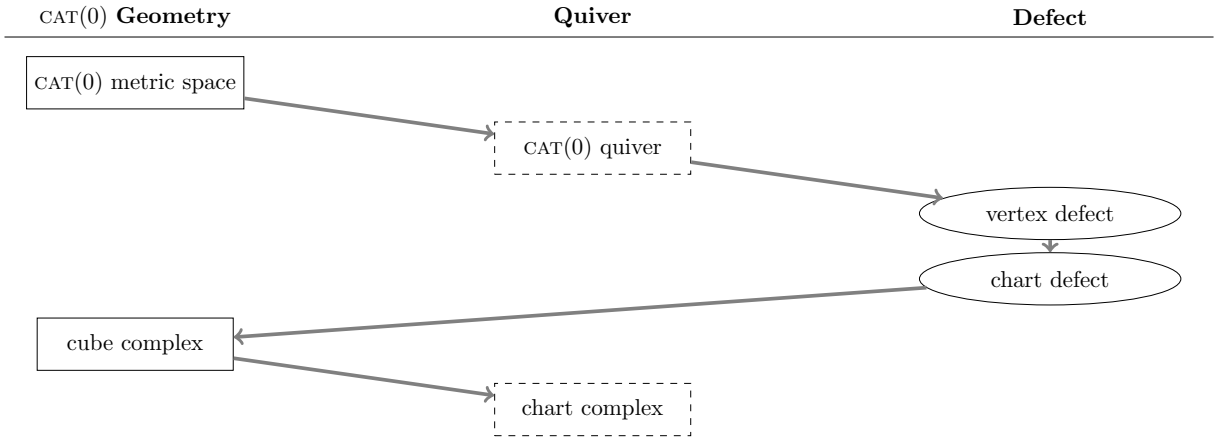

Figure 1: Organization of this thesis.

2 CAT(κ) geometry

In 1951, Alexandrov suggested that comparing triangles in an arbitrary metric space to those of a model space would give a notion of curvature [Ale51]. In this section I will present the concepts needed to formulate this relationship. Throughout this work (X, d) will denote a metric space and κ will be a real number.

2.1 Comparison of triangles

To define triangles in arbitrary spaces, we use the concept of *geodesic triangles*. Descriptively speaking, these are the triangles whose sides are "as straight as possible". More formally, a geodesic triangle can be defined from a geodesic segment.

Definition 2.1. *A* geodesic segment $[p, q]$ *with endpoints* p *and* q *(which in the case of geodesic triangles are the vertices of the triangle) is the image of a map* $c : [0, l] \to X$ *with* $c(0) = p$ *and* $c(l) = q$ *and* $d(c(t), c(t')) = |t' - t|$ *for all* $t, t' \in [0, l] \subset \mathbb{R}$ *with* d *being the metric of* (X, d)*. The map* c *defined in this way is a* geodesic.

In general, many geodesics may exist between two points. Thus, a geodesic segment is *not* uniquely determined by its endpoints.

Definition 2.2. *If all pairs of points* $x, y \in X$ *with* $d(x, y) < \delta$ *can be joined by a geodesic,* X *is said to be* δ-geodesic*. If this holds for all points* $x, y \in X$*, it is called a* geodesic metric space.

These concepts can then be used to define triangles:

Definition 2.3. *A* geodesic triangle $\Delta([p, q], [q, r], [r, p])$ *is given by three vertices* p, q, r *and sides* $[p, q], [q, r], [r, p]$ *being geodesic segments.*

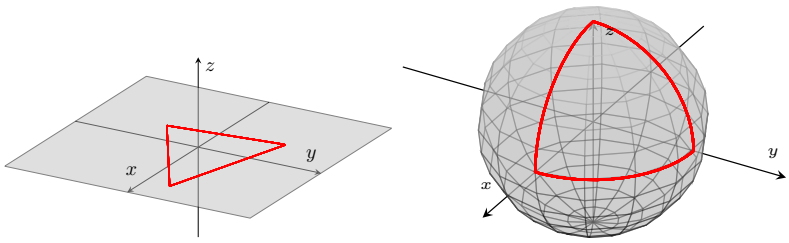

Figure 2: Geodesic triangles in Euclidean space (left) and on a sphere (right).

Hence, geodesic triangles will be given by the geodesic segments determining the sides. These triangles can then be compared to geodesic triangles with the same side lengths that lie in the so-called model spaces instead of X. These model spaces are metric spaces defined as follows. For a proof that the maps given here are indeed metrics, see pages 3, 16 and 20 of [BH99].

Definition 2.4. *The* model spaces (M_κ^n, d_κ) *used as a reference for the comparison are the metric spaces defined by*

$$M_\kappa^n := \begin{cases} \textit{hyperbolic space } \mathbb{H}^n = \{(u_1, ..., u_{n+1}) \in \mathbb{R}^{n+1} | \sum_{i=1}^{n} u_i^2 - u_{n+1}^2 = -1, u_{n+1} > 0\} & \textit{for } \kappa < 0 \\ \textit{Euclidean space } \mathbb{R}^n & \textit{for } \kappa = 0 \\ \textit{sphere } \mathbb{S}^n = \{(u_1, ..., u_{n+1}) \in \mathbb{R}^{n+1} | \sum_{i=1}^{n+1} u_i^2 = 1\} & \textit{for } \kappa > 0 \end{cases} \tag{1}$$

equipped with the metric d_κ *which for arbitrary* $x, y \in M_\kappa^n \subset \mathbb{R}^{n+1}$ *is given by* $d_0(x, y) = \left(\sum_{i=1}^{n} |x_i - y_i|\right)^{\frac{1}{2}}$ *(Euclidean metric) for* $\kappa = 0$ *and the unique solution of*

$$\cosh(\sqrt{-\kappa}\ d_\kappa(x, y)) = \sum_{i=1}^{n} x_i y_i - x_{n+1} y_{n+1}, \qquad 0 \le d_\kappa(x, y) \qquad \textit{for } \kappa < 0 \tag{2}$$

$$\cos(\sqrt{\kappa}\ d_\kappa(x, y)) = \sum_{i=1}^{n+1} x_i y_i, \qquad 0 \le \sqrt{\kappa}\ d_\kappa(x, y) \le \pi \qquad \textit{for } \kappa > 0 \tag{3}$$

otherwise. The maximal value of d_κ *gives the* diameter *of the metric space* M_κ^n*:*

$$D_\kappa := \begin{cases} \infty & \textit{for } \kappa \le 0 \\ \frac{\pi}{\sqrt{\kappa}} & \textit{for } \kappa > 0 \end{cases} \tag{4}$$

These model spaces are geodesic metric spaces. A geodesic segment $[x, y]$ in M_κ^n is unique if and only if $d_\kappa(x, y) < D_\kappa$ (cf. page 22 of [BH99]). Thus, geodesic triangles are uniquely defined by their vertices and will be denoted $\bar{\Delta} = \bar{\Delta}(\bar{p}, \bar{q}, \bar{r}) \subset M_\kappa^n$ for $\bar{p}, \bar{q}, \bar{r} \in M_\kappa^n$.

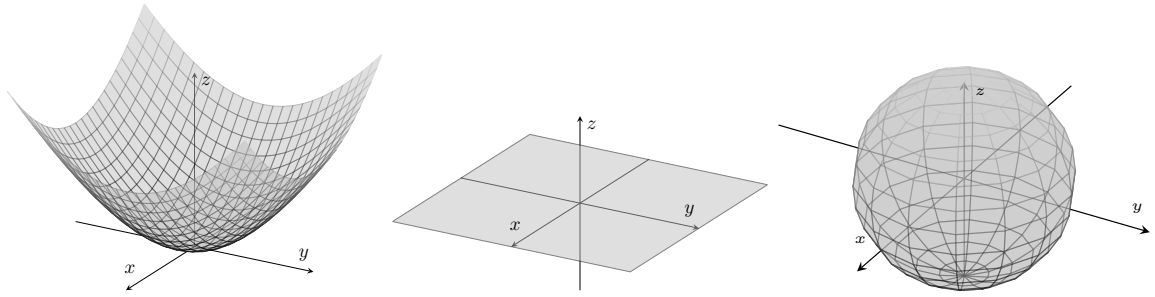

Figure 3: The model spaces for $\kappa = -1$ (left), $\kappa = 0$ (middle) and $\kappa = 1$ (right).

For analysing triangles in these model spaces, the following lemma provides a useful relationship between the lengths of the sides and one of the angles. It follows directly from the law of cosines in the corresponding metric spaces. For the proofs see pages 8, 17 and 20 of [BH99], a sketch is given in Fig. 4.

Lemma 2.5 (Law of Cosines)**.** *Consider a geodesic triangle in M_κ^n whose sides have positive lengths a, b, c and the angle between a and b is denoted γ. Then,*

$$\begin{aligned} \cosh(\sqrt{-\kappa}c) &= \cosh(\sqrt{-\kappa}a)\cosh(\sqrt{-\kappa}b) - \sinh(\sqrt{-\kappa}a)\sinh(\sqrt{-\kappa}b)\cos(\gamma) && \text{for } \kappa < 0 \\ c^2 &= a^2 + b^2 - 2ab\cos(\gamma) && \text{for } \kappa = 0 \\ \cos(\sqrt{\kappa}c) &= \cos(\sqrt{\kappa}a)\cos(\sqrt{\kappa}b) + \sin(\sqrt{\kappa}a)\sin(\sqrt{\kappa}b)\cos(\gamma) && \text{for } \kappa > 0 \end{aligned} \tag{5}$$

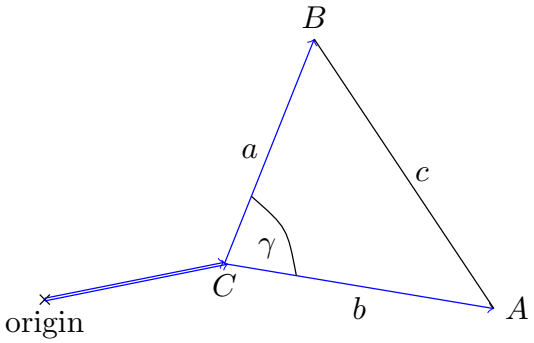

Figure 4: The law of cosines can be proven by considering the scalar product associated to the metric. This scalar product applied to the blue vectors can be related to the angle γ on the one hand side and the length of c on the other.

Definition 2.6. *For arbitrary $p, q, r \in X$, define the* perimeter *of a triangle Δ spanned by p, q, r to be $P_{p,q,r} = P_\Delta = d(p,q) + d(q,r) + d(r,p)$.*

For triangles in X with appropriate perimeter, the following lemma holds.

Lemma 2.7. *Let $p, q, r \in X$ and $P_{p,q,r} < 2D_\kappa$. Then exist $\bar{p}, \bar{q}, \bar{r} \in M_\kappa^2$ such that $d(p,q) = d_\kappa(\bar{p}, \bar{q})$, $d(q,r) = d_\kappa(\bar{q}, \bar{r})$, $d(r,p) = d_\kappa(\bar{r}, \bar{p})$. These points define a triangle $\bar{\Delta} = \bar{\Delta}(\bar{p}, \bar{q}, \bar{r}) \subset M_\kappa^2$ which is unique up to an isometry of M_κ^2.*

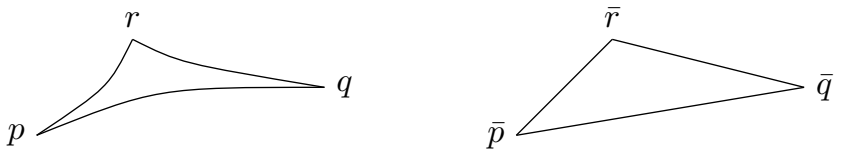

Figure 5: A geodesic triangle (left) in the metric space X and its comparison triangle (right) in Euclidean space.

This lemma motivates the definition of comparison triangles.

Definition 2.8. *The unique triangle $\bar{\Delta} = \bar{\Delta}(\bar{p}, \bar{q}, \bar{r}) \subset M_\kappa^2$ given by Lemma 2.7 is called a* comparison triangle *for the triple (p, q, r). For a geodesic triangle $\Delta = \Delta(p, q, r) \subset X$, $\bar{\Delta}$ is the* comparison triangle of Δ.

Proof. Following [BH99] for the proof of the existence, assume $d(p,q) \leq d(p,r) \leq d(q,r)$. To construct a triangle, fix a point $\bar{p} \in M_\kappa^2$ and calculate the angle $\gamma \in [0,\pi]$ opposite of $[q,r]$ from the law of cosines (Lemma 2.5). Then, choose geodesic segments $[\bar{p},\bar{q}]$ and $[\bar{p},\bar{r}]$ such that they are of lengths $d(p,q)$ and $d(p,r)$, respectively, and enclose an angle γ at $\bar{p}$. Define $\bar{q}$ and $\bar{r}$ to be the endpoints of the respective geodesic segments. From the triangle inequality one obtains $d(q,r) \leq d(p,q)+d(p,r)$, thus together with the inequality imposed on the perimeter of Δ, this results in $d(q,r) < D_\kappa$. Since M_κ^2 is D_κ-geodesic, there exists a geodesic segment $[\bar{q},\bar{r}]$. The resulting triangle $\bar{\Delta}(\bar{p},\bar{q},\bar{r})$ fulfills the conditions due to the law of cosines (Lemma 2.5).

For the uniqueness, assume $\bar{\Delta} = \bar{\Delta}(\bar{p},\bar{q},\bar{r})$ and $\hat{\Delta} = \hat{\Delta}(\hat{p},\hat{q},\hat{r})$ to be comparison triangles. Let $\gamma,\hat{\gamma}$ be the angles at the vertices $\bar{p},\hat{p}$ of $\bar{\Delta},\hat{\Delta}$, respectively. By the law of cosines (Lemma 2.5) and $\bar{\Delta},\hat{\Delta}$ being comparison triangles of a common original geodesic triangle, $\gamma = \hat{\gamma}$. Now consider $\bar{x} \in \bar{\Delta}$ and without loss of generality $\bar{x} \in [\bar{q},\bar{r}]$. Then define $\hat{x} \in [\hat{q},\hat{r}] \subseteq \hat{\Delta}$ such that $d_\kappa(\hat{q},\hat{x}) = d_\kappa(\bar{q},\bar{x})$ and $d_\kappa(\hat{r},\hat{x}) = d_\kappa(\bar{r},\bar{x})$. The law of cosines implies $d_\kappa(\hat{p},\hat{x}) = d_\kappa(\bar{p},\bar{x})$. Since this is possible for all $\bar{x} \in \bar{\Delta}$, the comparison triangles are isometric. □

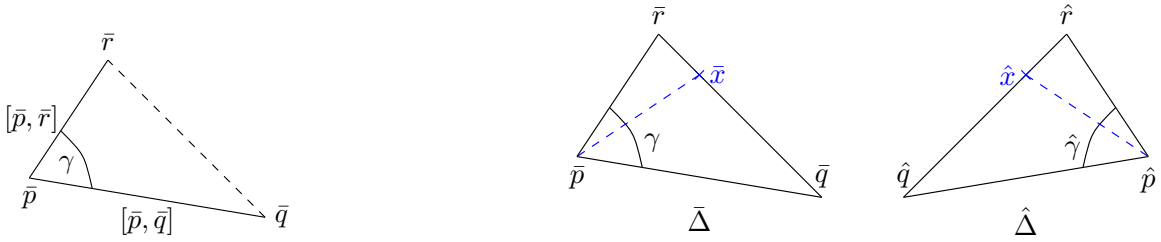

Figure 6: Idea of the proof of existence (left) and uniqueness (right) of comparison triangles (Lemma 2.7).

2.2 CAT(κ) inequality

Definition 2.9. *A geodesic triangle $\Delta \subset X$ with $P_\Delta < 2D_\kappa$ and comparison triangle $\bar{\Delta} \subset M_\kappa^2$ satisfies the* CAT(κ) inequality *if for all points $x,y \in \Delta$ and comparison points $\bar{x},\bar{y} \in \bar{\Delta}$*

$$d(x,y) \leq d_\kappa(\bar{x},\bar{y}) \tag{6}$$

holds.

Remark 2.10. The comparison points that this definition is refering to are defined by their distance to the vertices: Given $\Delta(p,q,r)$ with comparison triangle $\bar{\Delta}(\bar{p},\bar{q},\bar{r})$, a comparison point of $x \in [p,q]$ is the unique $\bar{x} \in [\bar{p},\bar{q}]$ that fulfills $d(\bar{x},\bar{p}) = d(x,p)$ and $d(\bar{x},\bar{q}) = d(x,q)$.

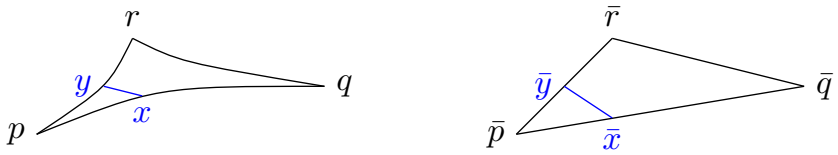

Figure 7: Comparison of points on a geodesic triangle (left) in the metric space X which is CAT(0) and on its comparison triangle (right) in Euclidean space.

Definition 2.11. *A metric space X is a* CAT(κ) *space if it satisfies the following two properties*

(i) X is D_κ-geodesic (for $\kappa \leq 0$, this is equivalent to X being a geodesic space)

(ii) all geodesic triangles $\Delta \subset X$ with $P_\Delta < 2D_\kappa$ satisfy the CAT(κ) *inequality (for $\kappa \leq 0$, this is equivalent to all geodesic triangles satisfying the inequality)*

Based on these definitions, Alexandrov introduced a notion of curvature related to the comparison of triangles [Ale51]:

Definition 2.12. *A metric space X which is locally* CAT(κ) *is said to have* curvature $K_{\text{CAT}} \leq \kappa$.

Lemma 2.13. *Let X be a D_κ-geodesic metric space that is* CAT(κ) *(Definition 2.11) and $\Delta = \Delta([p,q],[q,r],[r,p]) \subset X$ a geodesic triangle. For $x \in [p,q], x \neq p$ and $y \in [p,r], y \neq p$ follows that*

$$\alpha_{x,y} \leq \alpha_{q,r} \tag{7}$$

where $\alpha_{x,y}$ is the angle at $\bar{p}$ in the comparison triangle $\bar{\Delta} = \bar{\Delta}(\bar{p},\bar{x},\bar{y}) \subset M^2_\kappa$ and $\alpha_{q,r}$ analogously.

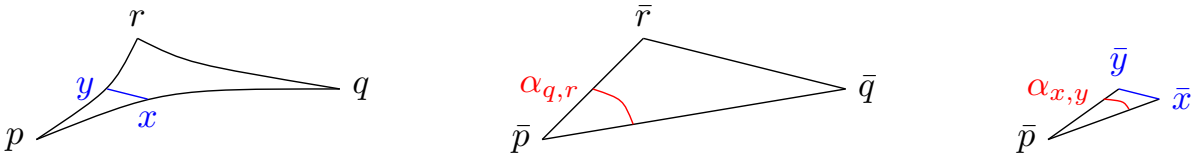

Figure 8: Comparison triangles used to state Lemma 2.13.

This lemma motivates the definition of angles in geodesic triangles in metric spaces:

Definition 2.14. *Let X be* CAT(κ) *and consider a triangle $\Delta = \Delta([p,q],[q,r],[r,p]) \in X$. For any two points $x \in [p,q], x \neq p$ and $y \in [p,r], y \neq p$ define the angle $\alpha_{x,y}$ as in Lemma 2.13. Then the limiting angle $\alpha_p = \lim_{x,y \to p} \alpha_{x,y}$ is called the* Alexandrov angle at p.

Proof. By construction of the comparison triangles,

$$d_\kappa(\bar{p},\bar{x}) = d(p,x) \leq d(p,q) = d_\kappa(\bar{p},\bar{q}) \tag{8}$$

$$d_\kappa(\bar{p},\bar{y}) = d(p,y) \leq d(p,r) = d_\kappa(\bar{p},\bar{r}) \tag{9}$$

On the other side, since $x, y \in \Delta$, the CAT(κ) inequality implies

$$d(x,y) = d_\kappa(\bar{x},\bar{y}) \leq d_\kappa(\bar{q},\bar{r}) \tag{10}$$

By the law of cosines (Lemma 2.5), this is equivalent to $\alpha_{x,y} \leq \alpha_{q,r}$. □

Corollary 2.15. *Let X be CAT(κ) and consider triangles as in Lemma 2.13. If $\Delta(\hat{p},\hat{q},\hat{r}) \subset M_\kappa^2$ a geodesic triangle (not necessarily a comparison triangle) with $d(p,q) = d_\kappa(\hat{p},\hat{q})$ and $d(p,r) = d_\kappa(\hat{p},\hat{r})$ and the angle γ at $\hat{p}$ satisfies $\gamma = \alpha_p$, then $d(q,r) \geq d_\kappa(\hat{q},\hat{r})$.*

This lemma and the previously stated results yield the following characterisations of the CAT(κ) condition [BH99].

Theorem 2.16. *Let $\kappa \in \mathbb{R}$ and X a D_κ-geodesic metric space. Then the following are equivalent:*

(i) X is CAT(κ) according to Definition 2.11.

(ii) For all geodesic triangles $\Delta([p,q],[q,r],[r,p]) \in X$ with $P_\Delta < 2D_\kappa$ and for all $x \in [q,r]$, the comparison point $\bar{x} \in [\bar{q},\bar{r}]$ in the comparison triangle $\bar{\Delta} = \bar{\Delta}(\bar{p},\bar{q},\bar{r}) \in M_\kappa^2$ satisfies $d(p,x) \leq d_\kappa(\bar{p},\bar{x})$.

(iii) For all geodesic triangles $\Delta([p,q],[q,r],[r,p]) \in X$ with $P_\Delta < 2D_\kappa$ and all $x \in [p,q], x \neq p$ and $y \in [p,r], y \neq p$, the angles defined as in Lemma 2.13 fulfill $\alpha_{x,y} \leq \alpha_{q,r}$.

(iv) For any geodesic triangle $\Delta \in X$ with $P_\Delta < 2D_\kappa$, the Alexandrov angle α_p at vertex p and the comparison angle $\gamma_{\bar{p}}$ at vertex $\bar{p}$ of the comparison triangle $\bar{\Delta} \in M_\kappa^2$ (which can be calculated by the law of cosines, Lemma 2.5) satisfy $\alpha_p \leq \gamma_{\bar{p}}$.

(v) For all non-degenerate geodesic triangles $\Delta = \Delta([p,q],[q,r],[r,p]) \in X$ with $P_\Delta < 2D_\kappa$, if $\hat{\Delta} = \hat{\Delta}(\hat{p},\hat{q},\hat{r}) \subset M_\kappa^2$ is a geodesic triangle (not necessarily a comparison triangle) with $d(p,q) = d_\kappa(\hat{p},\hat{q})$ and $d(p,r) = d_\kappa(\hat{p},\hat{r})$ and the angle γ at $\hat{p}$ equal to the Alexandrov angle α_p at vertex p of Δ, i.e. $\gamma = \alpha_p$, then $d(q,r) \geq d_\kappa(\hat{q},\hat{r})$.

Proof. Let $\Delta([p,q],[q,r],[r,p]) \subset X$ be a geodesic triangle with $P_\Delta < 2D_\kappa$ and comparison triangle $\bar{\Delta} = \bar{\Delta}(\bar{p},\bar{q},\bar{r}) \subset M_\kappa^2$.

(i) ⇒ (ii) follows directly from the CAT(κ) inequality.

(iv) ⇔ (v) can be proven using the law of cosines (Lemma 2.5) and solving the inequality for either the angles or the sides.

(iii) ⇒ (iv) is due to the definition of the Alexandrov angle (Corollary 2.15).

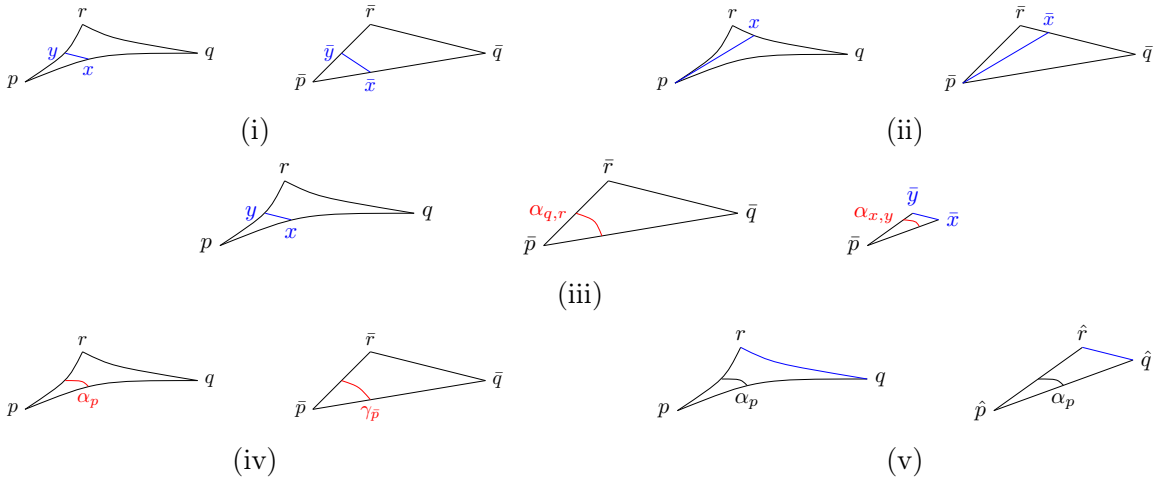

Figure 9: Characterisation of CAT(κ) spaces by arbitrary geodesic triangles. The numbering refers to the one in Theorem 2.16.

(i) $\Leftrightarrow$ (iii) follows from Lemma 2.13.

(ii) $\Rightarrow$ (iii) holds due to the following: Consider $\Delta([p,q],[q,r],[r,p]) \in X$ an arbitrary geodesic triangle with $P_\Delta < 2D_\kappa$. Fix $x \in [p,q], x \neq p$ and $y \in [p,r], y \neq p$ and denote $\alpha_{q,r}$ and $\alpha_{x,y}$ the angles at $\bar{p}$ in $\bar{\Delta}(\bar{p},\bar{q},\bar{r})$ and $\bar{\Delta}(\bar{p},\bar{x},\bar{y})$, respectively. Let $\bar{\Delta}^x = \bar{\Delta}(\bar{p}^x,\bar{x}^x,\bar{r}^x) \subset M^2_\kappa$ be a comparison triangle for $\Delta^x = \Delta(p,x,r) \subset X$ and $\alpha^x_{x,r}$ the angle at $\bar{p}^x$ in this triangle. This setting is shown in the upper part of Fig. 10. Since $y, r \in [p,r]$ with comparison points $\bar{y}^x, \bar{r}^x \in [\bar{p}^x, \bar{r}^x]$, (ii) implies $d_\kappa(\bar{x},\bar{y}) = d(x,y) \leq d_\kappa(\bar{x}^x,\bar{y}^x)$ and thus $\alpha_{q,r} \leq \alpha^x_{x,r}$ on the one hand and $d_\kappa(\bar{x}^x,\bar{r}^x) = d(x,r) \leq d_\kappa(\bar{x},\bar{r})$, i.e. $\alpha^x_{x,r} \leq \alpha_{q,r}$, on the other. Together, this yields $\alpha_{x,y} \leq \alpha_{q,r}$.

(iv) $\Rightarrow$ (ii) is proven true as follows: Fix $x \in [q,r], x \neq q,r$ with comparison point $\bar{x} \in [\bar{q},\bar{r}]$. Define $\hat{x} \in M^n_\kappa$ such that $\bar{\Delta}^r = \bar{\Delta}(\bar{p},\hat{x},\bar{r})$, $\bar{\Delta}^q = \bar{\Delta}(\bar{p},\bar{q},\hat{x}) \in M^2_\kappa$ are comparison triangles for $\Delta^r = \Delta(p,x,r)$, $\Delta^q = \Delta(p,q,x) \in X$, respectively. For a visualization see the lower part of Fig. 10. Denote γ the angle between $[\bar{q},\hat{x}]$ and $[\hat{x},\bar{r}]$ and δ the angle between $[\hat{x},\bar{r}]$ and $[\bar{r},\bar{q}]$. Then, $\delta + \beta_r = \beta$ where β_r, β are the angles at $\bar{r}$ in the triangles $\bar{\Delta}^r$ and $\bar{\Delta}$, respectively. Since $[q,r]$ is a geodesic segment, the Alexandrov angle between the parts of the segment $[q,x],[x,r] \subset [q,r]$ is $\alpha_x = \pi$ and (iv) implies $\gamma \geq \alpha_x = \pi$. Therefore, $\delta \geq 0$ which results in $\beta \geq \beta_r$. By the law of cosines (Lemma 2.5), $d_\kappa(\bar{p},\bar{x}) \geq d_\kappa(\bar{p},\hat{x}) = d(p,x)$ follows.

□

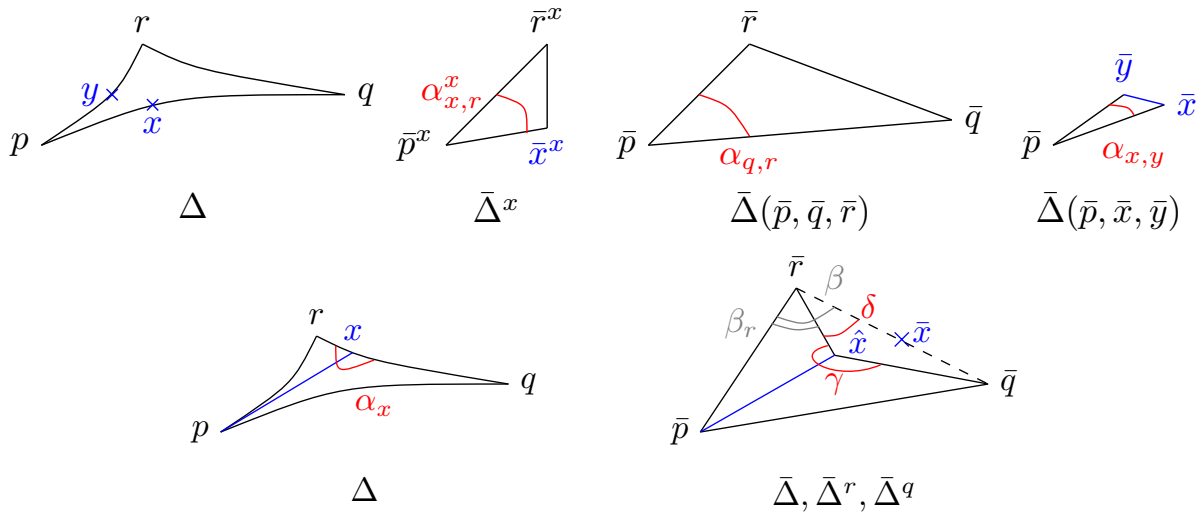

Figure 10: Triangles used in the proof of Theorem 2.16 for the implications "(ii) $\Rightarrow$ (iii)" (above) and "(iv) $\Rightarrow$ (ii)" (below).

2.3 Sectional curvature of CAT(κ) spaces

This section aims to relate the curvature K_{CAT} as defined in Definition 2.12 to the one known from Riemannian Geometry. In particular, this is done in terms of the sectional curvature. Throughout this section, let M be a Riemannian manifold and $\kappa \in \mathbb{R}$.

Theorem 2.17. *Let M be a smooth Riemannian manifold. Then M has curvature $K_{\text{CAT}} \leq \kappa$ as defined in Definition 2.12 if and only if its sectional curvature fulfills $K_{sect} \leq \kappa$, i.e. $K_{sect} \leq \kappa$ along all 2-planes in TM.*

The first implication was shown by Alexandrov [Ale51] while the second one was already proven by Cartan [Car25]. The proof given here follows the one given in [BH99]. For the first implication, consider the definition of the Alexandrov angle from Lemma 2.13 and the law of cosines in the model spaces (Lemma 2.5). Furthermore, the following lemma is helpful, which is proven in [Mey89], a sketch is given in Fig. 11.

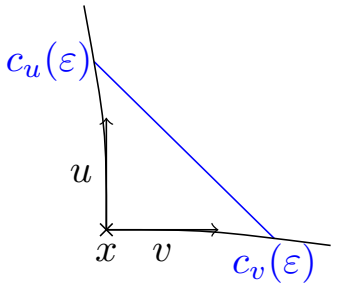

Figure 11: Lemma 2.18 can be proven by taking the Taylor series of the distance of $c_u(\varepsilon)$ and $c_v(\varepsilon)$ with the help of Jacobi fields. For a full proof see page 5 of [Mey89].

Lemma 2.18. *Let $u, v \in T_xM$ be orthogonal unit vectors for some $x \in M$ and c_u, c_v geodesics parametrized by arc-length with $c_u(0) = c_v(0) = x$ and $\dot{c}_u(0) = u, \dot{c}_v(0) = v$ in a sufficiently small neighbourhood of x, such that these geodesics are unique. Then,*

$$d(c_u(\varepsilon), c_v(\varepsilon))^2 = 2\varepsilon^2 - \frac{K_{sect}}{3}\varepsilon^4 + \mathcal{O}(\varepsilon^5) \tag{11}$$

where K_{sect} is the sectional curvature of M along the span of u, v in T_xM.

Proof of Theorem 2.17: $K_{\text{CAT}} \leq \kappa \Rightarrow K_{sect} \leq \kappa$. Let c_u and c_v geodesics in M as in Lemma 2.18 and $\varepsilon > 0$. Let Δ be the geodesic triangle with vertices $x, c_u(\varepsilon)$ and $c_v(\varepsilon)$ and the corresponding sides given by the geodesics c_u and c_v. Then the length of these two sides is ε by construction and the length of the third side is $A(\varepsilon) = d(c_u(\varepsilon), c_v(\varepsilon))$. By u, v being orthogonal, the Alexandrov angle between c_u and c_v is $\alpha = \frac{\pi}{2}$.

Now construct a corresponding geodesic triangle $\bar{\Delta} \subset M^2_\kappa$ with two sides having length ε that meet orthogonally. Let $B(\varepsilon)$ be the remaining side's length. By assumption, M has curvature $K_{\text{CAT}} \leq \kappa$, thus it is locally CAT(κ). Together with Corollary 2.15, this implies $A(\varepsilon) \geq B(\varepsilon)$. Furthermore, the law of cosines (Lemma 2.5) yields

$$\begin{aligned}
\cosh(\sqrt{-\kappa}A(\varepsilon)) \geq \cosh(\sqrt{-\kappa}B(\varepsilon)) = \cosh^2(\sqrt{-\kappa}\varepsilon) \qquad & \text{for } \kappa < 0 \\
A(\varepsilon)^2 \geq B(\varepsilon)^2 = 2\varepsilon^2 \qquad & \text{for } \kappa = 0 \\
\cos(\sqrt{\kappa}A(\varepsilon)) \leq \cos(\sqrt{\kappa}B(\varepsilon)) = \cos^2(\sqrt{\kappa}\varepsilon) \qquad & \text{for } \kappa > 0, \sqrt{\kappa}A(\varepsilon) \in [0, \pi]
\end{aligned} \tag{12}$$

Combining this with Lemma 2.18 and the appropriate Taylor series completes the proof:

$$\begin{aligned}
1 + (-\kappa)\left(\varepsilon^2 - \frac{K_{sect}}{6}\varepsilon^4\right) + \frac{\kappa^2}{6}\varepsilon^4 + \mathcal{O}(\varepsilon^5) \geq 1 + (-\kappa)\varepsilon^2 + \frac{\kappa^2}{3}\varepsilon^4 + \mathcal{O}(\varepsilon^5) \qquad & \text{for } \kappa < 0 \\
2\varepsilon^2 - \frac{K_{sect}}{6}\varepsilon^4 + \mathcal{O}(\varepsilon^5) \geq 2\varepsilon^2 \qquad & \text{for } \kappa = 0 \\
1 - \kappa\left(\varepsilon^2 - \frac{K_{sect}}{6}\varepsilon^4\right) + \frac{\kappa^2}{6}\varepsilon^4 + \mathcal{O}(\varepsilon^5) \leq 1 - \kappa\varepsilon^2 + \frac{\kappa^2}{3}\varepsilon^4 + \mathcal{O}(\varepsilon^5) \qquad & \text{for } \kappa > 0
\end{aligned} \tag{13}$$

yields $K_{sect} \leq \kappa$ in any case. □

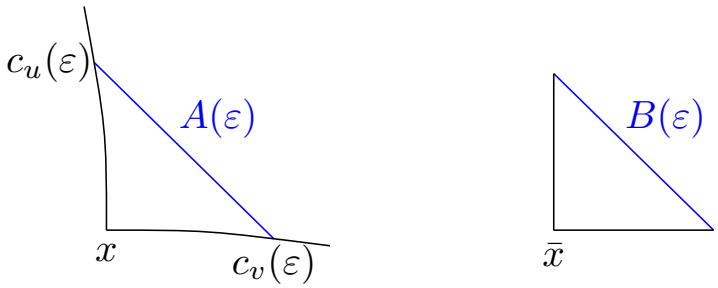

Figure 12: Setting to prove the first implication of Theorem 2.17.

For the second implication we will need the following lemmas.

Lemma 2.19. *Let $p \in M$ (which is a Riemannian manifold), $o \in M^n_\kappa$ and $\epsilon > 0$ such that for all $x \in B(p, \frac{\epsilon}{2})$ there exists a map $f_x : B(o, \epsilon) \to B(x, \epsilon)$ for which the following conditions hold:*

(i) $f_x(o) = x$

(ii) its differential satisfies $|D_y f_x(v)| \geq |v|$ *for all* $y \in B(o, \epsilon)$ *and* $v \in T_y M^n_\kappa$

(iii) in condition (ii), equality holds if v is tangent to the geodesic through o and y (i.e. $D_o f_x$ is an isometry)

Then $B(p, \frac{\epsilon}{2})$ is CAT(κ).

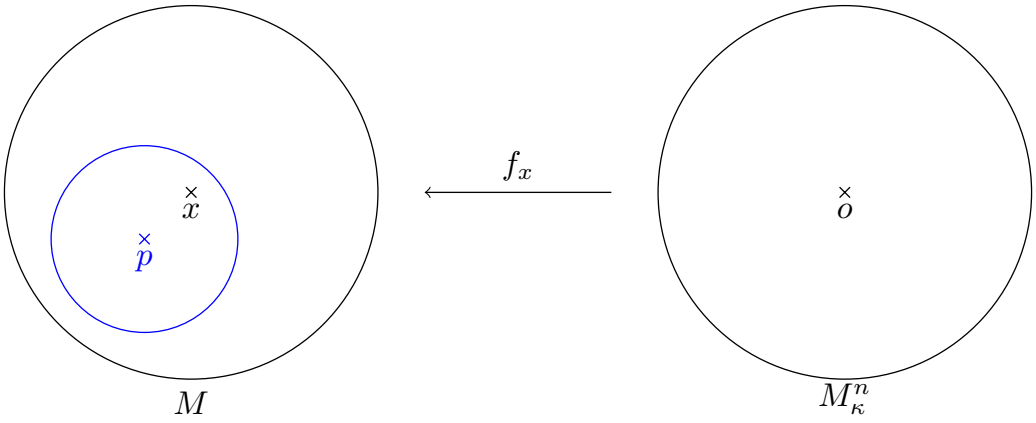

Figure 13: Setting of Lemma 2.19. The blue ball is the one that ends up being CAT(κ).

Proof. Fix $x \in B(p, \frac{\epsilon}{2})$. By assumption, for any curve $c : [0, 1] \to B(o, \epsilon)$ that is piecewise C^1 and l_R being the Riemannian length, $l_R(f_x \circ c) \geq l_R(c)$ holds. For the geodesic c through o and y, equality holds. The image of this geodesic segment $[o, y]$ under f_x is the unique geodesic segment $[x, f_x(y)]$.

Now, consider $y, z \in B(o, \frac{\epsilon}{2})$. By definition, $d(f_x(y), f_x(z))$ is given by the infimum of lengths of piecewise C^1 curves that join $f_x(y)$ and $f_x(z)$. For any such curve C exists a piecewise C^1 curve c joining y and z, such that $C = f_x \circ c$. As stated before, $l_R(c) \leq l_R(C)$ and thus $d(y, z) \leq d(f_x(y), f_x(z))$.

This implies that for any non-degenerate triangle $\Delta \subseteq B(p, \frac{\epsilon}{2})$ the angles at its vertices are less or equal to the ones in the comparison triangle $\bar{\Delta} \subseteq B(o, \epsilon) \subseteq M^n_\kappa$. By Theorem 2.16, this concludes the proof. □

Lemma 2.20. *Let M be smooth enough (C^3) and have sectional curvature $K_{sect} \leq \kappa$. Then, for all $p \in M$ one can find a neighbourhood $V \ni p$ and $\epsilon > 0$ in a way that for every $x \in V$ there is a map $f : B(o, \epsilon) \to M$ as in Lemma 2.19.*

Proof. Fix $p \in V \subset M$. In a compact subset of V containing p exists $\epsilon > 0$ such that for any x in this set the exponential map $\exp_x : T_x M \to B(x, \epsilon)$ is a well defined diffeomorphism. Now fix such an x and an $o \in M^n_\kappa$. Since $T_o M^n_\kappa$ and $T_x M$ can be identified, define

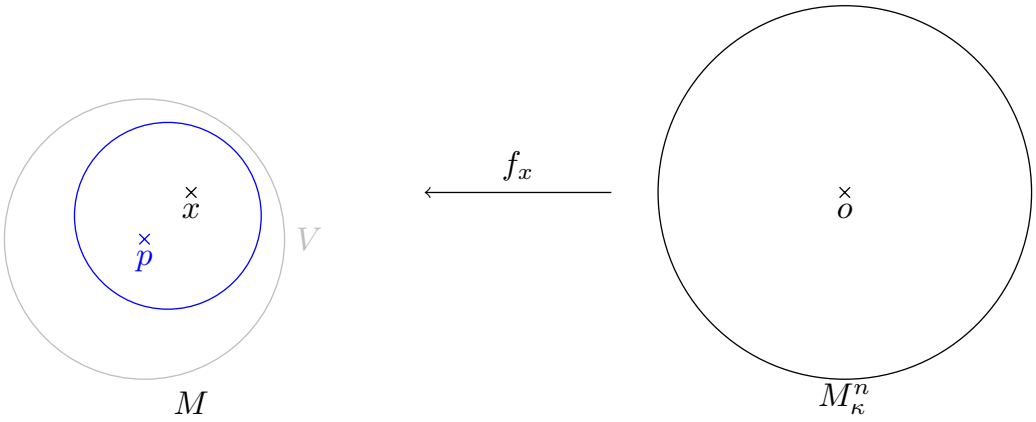

Figure 14: Setting of Lemma 2.20. The neighbourhood V is shown in grey and the compact subset in blue.

$f = \exp_x \circ \exp_o^{-1}$. This map satisfies the equality for tangents of geodesics as required in Lemma 2.19 and $f(o) = x$.

To show that the differential of f also satisfies the inequality, consider two Jacobi fields: $J_o(t)$ being associated to the one-parameter family $c(t) = \exp_o(t(u + sv))$ and $J_x(t)$ being associated to $\exp_x(t(u + sv))$. By construction of f, its differential maps J_o onto J_x. Furthermore, define $j_\kappa(t)$ to be the solution of the differential equation $j''_\kappa(t) = -\kappa j_\kappa(t)$. The differential equation for Jacobi fields and $J_x(t)$ in particular gives is $|J_x|''(t) \geq K_{sect}(t)|J_x|(t)$ with $K_{sect}(t)$ being the sectional curvature along $c(t)$. Hence, one obtains $|J_x|(t) \geq j_\kappa(t)$. On the other hand, by construction of J_o from the exponential map and due to the Riemannian metric on M^2_κ, $j_\kappa(t) = |J_o|(t)$ holds. This implies $|J_x|(t) \geq |J_o|(t)$ which concludes the proof. □

Proof of Theorem 2.17: $K_{sect} \leq \kappa \Rightarrow K_{\text{CAT}} \leq \kappa$. By hypothesis, M is a smooth manifold with $K_{sect} \leq \kappa$. With Lemma 2.20 one obtains a suitable function f to apply Lemma 2.19, thus M is locally CAT(κ) and hence $K_{\text{CAT}} \leq \kappa$. □

3 Discrete CAT(0) geometry

The idea of describing curvature by comparing triangles can also be applied to discrete lattices, where defects can be characterized based on a similar procedure. The description of the quivers is based on the language developed by Taliesin Beynon and myself [Bey21; Sei21]. We consider quivers defined in the following way:

Definition 3.1. *Let $\mathcal{Q}$ be a graph whose edges are labelled with symbols and have a specified direction. Then $\mathcal{Q}$ is called a* cardinal quiver *or* quiver *if it satisfies the following* local uniqueness property*: For each vertex v of $\mathcal{Q}$ and a given symbol and a direction ("incident to v" or "emergent from v"), there exists at most one edge that is both labelled with this symbol and has the specified direction. In this sense, the tuples* (symbol, direction) *are locally unique.*

For talking about these quivers, a second definition is helpful:

Definition 3.2. *Given a quiver $\mathcal{Q}$, the tuple* (symbol, direction) *used to label an edge is called* cardinal*. Instead of following an edge labelled by a cardinal $\mathtt{b} = \blacktriangle = (\bullet, \uparrow)$ in the original direction, we can also consider its inverse which is denoted by $\mathtt{b}^* = \blacktriangledown = (\bullet, \downarrow)$.*

Remark 3.3. Loops and multiple edges between vertices of the quiver $\mathcal{Q}$ are allowed. By the local uniqueness property, multiple edges between two vertices must be labelled with different cardinals. For more compact notation, we identify them with one edge with two cardinals.

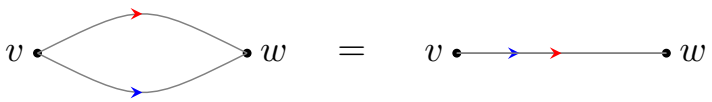

Figure 15: Illustration of multiple edges between vertices v, w as described in Remark 3.3.

3.1 Model lattice and metric

In this section, we restrict to the comparison with the planar case, i.e. CAT(0) geometry. In the discrete and two-dimensional analog, this refers to the comparison with the square lattice. Throughout the section, let $\mathcal{Q}$ be a quiver.

Definition 3.4. *Let v be a vertex on $\mathcal{Q}$ on which cardinals $\mathtt{a}_1, ..., \mathtt{a}_n$ are defined. Then the combination $\mathtt{P} = \mathtt{c}_1 ... \mathtt{c}_k$ of cardinals $\mathtt{c}_i \in \{\mathtt{a}_1, ..., \mathtt{a}_n, \mathtt{a}_1^*, ..., \mathtt{a}_n^*\}$ is called a* pathword*. If by starting at v and following $\mathtt{c}_1 ... \mathtt{c}_k$ one after the other, a vertex of $\mathcal{Q}$ is reached, define this to be w. Then the* path *c starting at v and following $\mathtt{P}$ to the vertex w is denoted by $c = (v : \mathtt{P} : w)$.*

Definition 3.5. *Consider two vertices x and y on $\mathcal{Q}$ on which cardinals $\mathtt{a}_1, ..., \mathtt{a}_n$ are defined. Then consider a path $c = (x : \mathtt{P} : y)$ as in Definition 3.4. Its pathword can be decomposed into k cardinals $\mathtt{c}_i \in \{\mathtt{a}_1, ..., \mathtt{a}_n, \mathtt{a}_1^*, ..., \mathtt{a}_n^*\}$ for $i = 1, ..., k$ such that $\mathtt{P} = \mathtt{c}_1 ... \mathtt{c}_k$. Define the* length of path *as the* length of pathword *of that path by*

$$l(c) = l(\mathtt{c}_1 ... \mathtt{c}_k) = k \tag{14}$$

which is the total count of cardinals. Furthermore, for any cardinal $\mathtt{b} \in \{\mathtt{a}_1, ..., \mathtt{a}_n, \mathtt{a}_1^*, ..., \mathtt{a}_n^*\}$ defined on $\mathcal{Q}$, define its multiplicity *in the pathword $\mathtt{P}$ to be*

$$n_{\mathtt{b}} = n_{\mathtt{b}}(\mathtt{P}) = \sum_{i=1}^{k} \delta_{\mathtt{c}_i, \mathtt{b}} \tag{15}$$

where $\delta_{\mathtt{a},\mathtt{b}} = \begin{cases} 1 & \mathtt{a} = \mathtt{b} \\ 0 & \mathtt{a} \neq \mathtt{b} \end{cases}$ *is the Kronecker-Delta.*

Definition 3.6. *Consider a quiver $\mathcal{L}$ with vertex set $V = \mathbb{Z}^2$ and for each $(n, m) \in V$ define two edges starting at that vertex: The edge from (n, m) to $(n + 1, m)$ is labelled by a cardinal $\mathtt{x}$ and the edge from (n, m) to $(n, m + 1)$ is labelled by a different cardinal $\mathtt{y}$. The resulting quiver is called a square lattice and is shown in Fig. 16.*

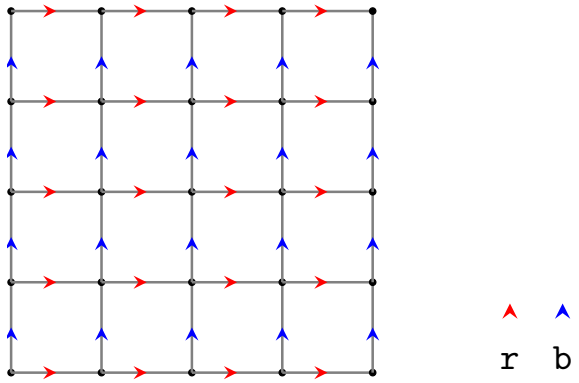

Figure 16: A section of the square lattice $\mathcal{L}$ defined in Definition 3.6. The lattice continues to infinity at either side although this cannot be displayed here.

Example 3.7. (i) The paths shown in Fig. 17 have lengths $l(c_1) = 3$ and $l(c_2) = 2$. For the concatenation, $l((x : \mathtt{brrb}^*\mathtt{b}^* : y)) = l(c_1 \cdot c_2) = l(c_1) + l(c_2) = 5$ holds.

(ii) Since a path c and its inverse c^* have the same amount of cardinals, $l(c) = l(c^*)$.

(iii) In general, for two paths $c = (x : \mathtt{P} : y)$ and $b = (y : \mathtt{R} : z)$, the length of the path composition is given by $l(c \cdot d) = l(c) + l(d)$.

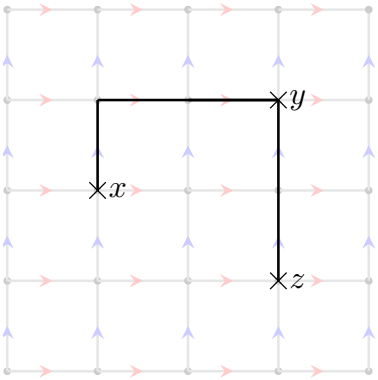

Figure 17: Paths $c_1 = (x : \texttt{brr} : y)$ and $c_2 = (y : \texttt{b}^*\texttt{b}^* : z)$.

(iv) For a quiver with cardinal $\texttt{c}$, the path $c = (x : \texttt{cc}^*\texttt{cc}^*\texttt{cc}^* : x)$ has length of path $l(c) = 6$ by the above definition. Another possible definition would be to consider the set of pathwords as a group, the so-called *word group* described by [Bey21]. Then consecutive cardinals would cancel and yield the word metric $l_{word}(c) = 0$. However, this definition is not useful for the definition of geodesics as in Definition 3.9.

Lemma 3.8. *Consider $V(\mathcal{Q})$ the set of vertices of $\mathcal{Q}$. Then the map*

$$\begin{aligned} d : V(\mathcal{Q}) \times V(\mathcal{Q}) &\to \mathbb{R} \\ (x, y) &\mapsto \inf_{c \text{ path from } x \text{ to } y} l(c) \end{aligned} \tag{16}$$

is a metric on $\mathcal{Q}$.

Due to the discreteness of $\mathcal{Q}$, the infimum in the definition of d in Lemma 3.8 is in fact a minimum. This gives rise to the following definition:

Definition 3.9. *In analogy to metric spaces, we call the path which minimizes the metric a* geodesic. *Its pathword is called a* minimal pathword.

Proof. Verify positive definiteness, symmetry and the triangle inequality for the map d:

(i) $d(x, y) \geq 0$ holds for all $x, y \in V(\mathcal{Q})$ since $l(c) \geq 0$ for all paths on $\mathcal{Q}$. This is due any pathword being given by a positive number of cardinals. $d(x, y)$ vanishes if and only if a path c exists which connects x to y and satisfies $l(c) = 0$. This is equivalent to the pathword of c being empty, thus $c = (x :: y) = (x :: x)$ and $x = y$.

(ii) Fix x, y vertices of $\mathcal{Q}$. Then $d(x, y) = \min_{c \text{ path from } x \text{ to } y} l(c)$, thus exists a path $c_{min} = (x : \texttt{P}_{min} : y)$ from x to y with minimal length. Inverting this path gives $c^*_{min} = (y : \texttt{P}^*_{min} : x)$, where the inverted pathword $\texttt{P}^*_{min}$ is given by the inverted cardinals of $\texttt{P}_{min}$ in reversed order. As remarked in (ii) of Example 3.7, $l(c) = l(c^*)$, thus c^*_{min} minimizes the length of paths from y to x. Hence, $d(y, x) = \min_{c \text{ path from } y \text{ to } x} l(c) = \min_{c \text{ path from } x \text{ to } y} l(c^*) = \min_{c \text{ path from } x \text{ to } y} l(c) = d(x, y)$.

(iii) Let x, y, z be vertices of $\mathcal{Q}$. Due to the infimum in the definition of the metric being a minimum exist paths $c_{min} = (x : \mathtt{P}_{min} : y)$ and $b_{min} = (y : \mathtt{R}_{min} : z)$ minimizing the lengths of paths from x to y and y to z, respectively. This implies $d(x,y) + d(y,z) = l(c_{min}) + l(b_{min}) = l(c_{min} \cdot d_{min}) \geq \min_{a \text{ path from } x \text{ to } z} l(a) = d(x,z)$ as $c_{min} \cdot d_{min}$ is a path from x to z.

Since all three conditions are met, d is a metric on $\mathcal{Q}$. □

Remark 3.10. If we want to highlight the metric defined on a quiver $\mathcal{Q}$, we write $(\mathcal{Q}, d_{\mathcal{Q}})$. If not specified further, this metric is the one constructed in Lemma 3.8.

Corollary 3.11. *For d defined as in Lemma 3.8, $(\mathcal{Q}, d)$ is a geodesic metric space.*

Remark 3.12. The metric space defined in this way is not uniquely geodesic: In particular, consider a square lattice $\mathcal{L}$ with cardinals $\mathtt{a}, \mathtt{b}$ and x a vertex on $\mathcal{Q}$. Let y be the ending vertex of the path $c = (x : \mathtt{ab} : y)$. By Definition 3.5, $l(c) = 2$ and since no shorter path from x to y can be found, c is a geodesic. However, $\tilde{c} = (x : \mathtt{ba} : y) \neq c$ has length $l(\tilde{c}) = 2$ and is thus a geodesic, too.

Definition 3.13. *Let $(\mathcal{Q}, d)$ a geodesic metric space on the quiver $\mathcal{Q}$ as in Corollary 3.11. A* geodesic triangle $\Delta = \Delta([p,q],[q,r],[r,p])$ *on the quiver $\mathcal{Q}$ is given by three vertices p, q, r of $\mathcal{Q}$ and the sides $[p,q],[q,r],[r,p]$ being geodesics in the sense of the metric d.*

3.2 Square lattices with vertex defects

To investigate CAT(0) geometry on quivers, we have a closer look at square lattices. In this section, $\mathcal{L}$ will always denote a square lattice as given in Definition 3.6 and $\mathcal{D}$ will be a square lattice with vertex defects which is defined as follows:

Definition 3.14. *Vertices that are introduced additionally into or deleted from a square lattice $\mathcal{L}$ are called* positive *or* negative vertex defect*, respectively (Fig. 18). The resulting quiver $\mathcal{D}$ is a* square lattice with vertex defects *or simply a* square lattice with defects*.*

In the discrete setting, the finite number of cardinals in the circumference of a geodesic triangle (Definition 3.13) affects the properties of the triangle. This motivates the following definition:

Definition 3.15. *Consider a geodesic triangle Δ on a square lattice with defects $\mathcal{D}$. Let c be the path that gives the circumference of this triangle. If for any cardinal $\mathtt{a}$ in the pathword of c, its multiplicity and the one of its inverse are equal, $n_{\mathtt{a}} = n_{\mathtt{a}^*}$, Δ is called a* lattice geodesic triangle*.*

Remark 3.16. All triangles on a square lattice $\mathcal{L}$ are lattice ones since their circumference needs to be closed. On a square lattice with cardinals $\mathtt{x}$ and $\mathtt{y}$ a path is closed if and only if the occurrences of cardinals and inverted cardinals in its pathword satisfy $n_{\mathtt{x}} = n_{\mathtt{x}^*}$ and $n_{\mathtt{y}} = n_{\mathtt{y}^*}$.

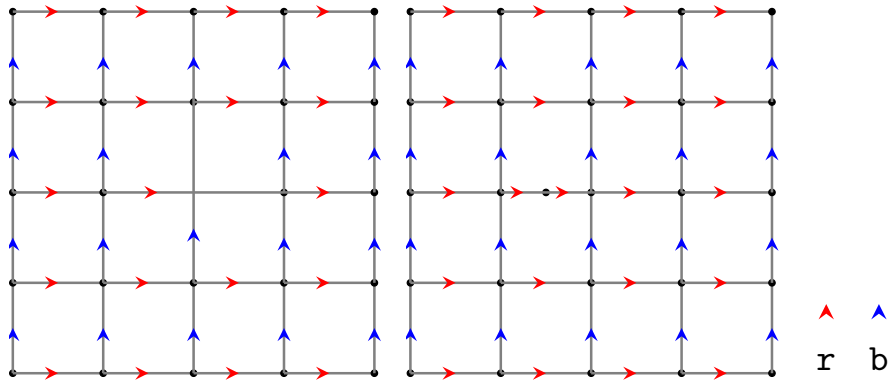

Figure 18: Sections of a square lattice with cardinals r and b where one vertex is missing (negative vertex defect, left) or was added (positive vertex defect, right).

To establish a notion of CAT(0) geometry on quivers, we need to define comparison triangles. Descriptively speaking, the comparison triangle of some triangle Δ in a square lattice with defects should look the same as Δ but without the vertex defects. One possibility is to consider a mapping of cardinals and to define the comparison triangle by using the images of the pathwords of the geodesic segments under this mapping. This can be formalized as follows:

Definition 3.17. *Let $\mathcal{Q}$ and $\mathcal{R}$ be two quivers with cardinals $\mathtt{q}_i, i \in I$ and $\mathtt{r}_j, j \in J$, respectively, for I, J index sets. Then a bijection $\varphi : \{\mathtt{q}_i \mid i \in I\} \to \{\mathtt{r}_j \mid j \in J\}$ is called a* cardinal transfomation *from $\mathcal{Q}$ to $\mathcal{R}$.*

Remark 3.18. The square lattice given by Definition 3.6 is unique up to cardinal transformation.

Definition 3.19. *Considering two quivers $\mathcal{Q}$ and $\mathcal{R}$ and geodesic triangles $\Delta_\mathcal{Q}, \Delta_\mathcal{R}$ on them, then $\Delta_\mathcal{Q}$ is* congruent *to $\Delta_\mathcal{R}$ if exists a cardinal transformation φ from $\mathcal{Q}$ to $\mathcal{R}$ such that the pathwords of the geodesic segments that are the edges of $\Delta_\mathcal{Q}$ can be transformed into the ones of $\Delta_\mathcal{R}$ by cardinal-wise application of φ.*

Lemma 3.20. *For a quiver $\mathcal{Q}$, congruency is an equivalence relation on the set of triangles on $\mathcal{Q}$.*

Proof. Check reflexivity, symmetry and transitivity:

(i) Let Δ be a geodesic triangle on $\mathcal{Q}$. Then Δ is trivially congruent to Δ by using the identity as the cardinal transformation.

(ii) Given $\Delta, \tilde{\Delta}$ triangles on $\mathcal{Q}$ and Δ congruent to $\tilde{\Delta}$ by the cardinal transformation φ, one obtains that φ^{-1} is a cardinal transformation from $\mathcal{Q}$ to $\mathcal{Q}$, too, which implies that $\tilde{\Delta}$ is congruent to Δ.

(iii) Consider the following geodesic triangles on $\mathcal{Q}$: Δ which is congruent to $\tilde{\Delta}$ by the cardinal transformation φ and $\hat{\Delta}$ which is congruent to $\tilde{\Delta}$ by ψ. Then $\psi \circ \varphi$ is a cardinal transformation as well and hence Δ is congruent to $\hat{\Delta}$.

Since all three conditions hold, congruency is an equivalence relation. □

Lemma 3.21. *Consider a square lattice $(\mathcal{L}, d_{\mathcal{L}})$ and a square lattice with defects $(\mathcal{D}, d_{\mathcal{D}})$. Let $\Delta = \Delta(p, q, r)$ be a lattice geodesic triangle on $\mathcal{D}$. Then there exist vertices $\bar{p}, \bar{q}, \bar{r}$ and a triangle $\bar{\Delta} = \bar{\Delta}(\bar{p}, \bar{q}, \bar{r})$ in $\mathcal{L}$ that is congruent to Δ. $\bar{\Delta}$ is unique up to congruency.*

Definition 3.22. *For a square lattice with defects $(\mathcal{D}, d_{\mathcal{D}})$ and a lattice geodesic triangle Δ on it, the triangle $\bar{\Delta} = \bar{\Delta}(\bar{p}, \bar{q}, \bar{r})$ in $\mathcal{L}$ defined by $\bar{p}, \bar{q}, \bar{r}$ as in Lemma 3.21 is called the* comparison triangle *of Δ.*

Remark 3.23. Since the count of cardinals in the pathwords of the geodesic segments is not changed by the cardinal transformation used for the congruency, the lengths of the geodesic segments in congruent triangles are the same. Thus, the same holds for a triangle and its comparison triangle. In the setting of Lemma 3.21, this means $d_{\mathcal{D}}(p, q) = d_{\mathcal{L}}(\bar{p}, \bar{q})$, $d_{\mathcal{D}}(q, r) = d_{\mathcal{L}}(\bar{q}, \bar{r})$, $d_{\mathcal{D}}(r, p) = d_{\mathcal{L}}(\bar{r}, \bar{p})$.

Proof. Let $(\mathcal{L}, d_{\mathcal{L}})$, $(\mathcal{D}, d_{\mathcal{D}})$ as in Lemma 3.21 and $\Delta = \Delta(p, q, r)$ a geodesic triangle in $\mathcal{D}$ with edges $[p, q] = (p : \mathtt{a}_1 ... \mathtt{a}_k : q)$, $[q, r] = (q : \mathtt{a}_{k+1} ... \mathtt{a}_l : r)$, $[r, p] = (r : \mathtt{a}_{l+1} ... \mathtt{a}_n : p)$ where $\mathtt{a}_1, ..., \mathtt{a}_n$ are (possibly inverted) cardinals of $\mathcal{D}$. Choose $\bar{p}$ vertex of $\mathcal{L}$ and φ a cardinal transformation from $\mathcal{D}$ to $\mathcal{L}$. Then define the vertices $\bar{q}, \bar{r}$ and the geodesic segments between them by $[\bar{p}, \bar{q}] = (\bar{p} : \varphi(\mathtt{a}_1) ... \varphi(\mathtt{a}_k) : \bar{q})$, $[\bar{q}, \bar{r}] = (\bar{q} : \varphi(\mathtt{a}_{k+1}) ... \varphi(\mathtt{a}_l) : \bar{r})$, $[\bar{r}, \bar{p}] = (\bar{r} : \varphi(\mathtt{a}_{l+1}) ... \varphi(\mathtt{a}_n) : \bar{p})$. The last one is well-defined since Δ is a lattice geodesic triangle. Thus, the triangle $\bar{\Delta}$ given by these geodesic segments is well-defined, too, and it is congruent to Δ by construction. The uniqueness follows from congruency being an equivalence relation (Lemma 3.20). □

Definition 3.24. *A lattice geodesic triangle Δ in the square lattice with defects $(\mathcal{D}, d_{\mathcal{D}})$ with comparison triangle $\bar{\Delta}$ in the square lattice $(\mathcal{L}, d_{\mathcal{L}})$ satisfies the* discrete CAT(0) inequality *if for all points $x, y \in \Delta$ and comparison points $\bar{x}, \bar{y} \in \bar{\Delta}$ holds the following:*

$$d_{\mathcal{D}}(x, y) \leq d_{\mathcal{L}}(\bar{x}, \bar{y}) \tag{17}$$

If this is the case for all lattice geodesic triangles on $\mathcal{D}$, the quiver $\mathcal{D}$ is said to satisfy the discrete CAT(0) *inequality.*

Remark 3.25. The comparison points $\bar{x}, \bar{y}$ refered to in this definition are obtained by transferring the sides of Δ and thus the paths from the neighbouring vertices to x or y to the square lattice $\mathcal{L}$ by cardinal transformation.

Lemma 3.26. *Consider a lattice geodesic triangle Δ in $\mathcal{D}$ such that Δ encloses exactly one vertex defect. If this is a positive vertex defect,*

$$d_{\mathcal{D}}(x, y) \geq d_{\mathcal{L}}(\bar{x}, \bar{y}) \tag{18}$$

holds for all points x, y of the triangle Δ and comparison points $\bar{x}, \bar{y}$ of its comparison triangle $\bar{\Delta}$ in the square lattice $(\mathcal{L}, d_{\mathcal{L}})$. The discrete CAT(0) *inequality does not hold in this case.*

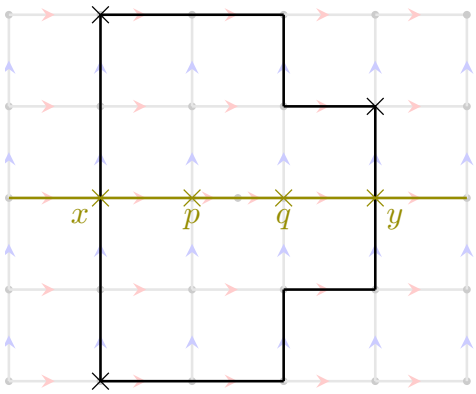

Figure 19: Setup for the ">"-part of the proof of Lemma 3.26 for $\mathtt{a} = \mathtt{r}$. The marked geodesic is given by the pathword $\mathtt{r}^n$ and is the extension of the edge $p : \mathtt{rr} : q$ where the vertex defect was introduced.

Proof. Let $\bar{\Delta}$ in the square lattice $\mathcal{L}$ be a comparison triangle for Δ in $\mathcal{D}$. Consider x, y to be vertices on Δ and $[x, y]$ to denote a geodesic segment between them. The comparison vertices are $\bar{x}, \bar{y}$ and are joined by the geodesic segment $[\bar{x}, \bar{y}]$. Let $(x : \mathtt{P} : y)$ be the path obtained from $[\bar{x}, \bar{y}]$ by going from $\mathcal{L}$ to $\mathcal{D}$, i.e. by introducing an additional vertex. If this additional vertex does not lie on $(x : \mathtt{P} : y)$, its length minimizing property remains unchanged and thus $(x : \mathtt{P} : y) = [x, y]$, i.e. $d_{\mathcal{D}}(x, y) = l([x, y]) = l([\bar{x}, \bar{y}]) = d_{\mathcal{L}}(\bar{x}, \bar{y})$ holds.

Now assume the additional vertex to be located on $(x : \mathtt{P} : y)$. This enhances the number of vertices and thus edges on this path, hence the number of cardinals in the pathword increases. If the resulting path $(x : \mathtt{P} : y)$ still minimizes the length, this implies $d_{\mathcal{D}}(x, y) = l([x, y]) = l((x : \mathtt{P} : y)) \geq l([\bar{x}, \bar{y}]) = d_{\mathcal{L}}(\bar{x}, \bar{y})$.

In the opposite case, i.e. if exists a path $(x : \mathtt{Q} : y) = [x, y]$ with minimal length and $l((x : \mathtt{P} : y)) > l((x : \mathtt{Q} : y))$, consider its comparison path $(\bar{x} : \mathtt{Q} : \bar{y})$ in $\mathcal{L}$. Since the additional vertex is located on $(x : \mathtt{P} : y)$ instead of $(x : \mathtt{Q} : y)$, this results in $d_{\mathcal{D}}(x, y) = l([x, y]) = l((x : \mathtt{Q} : y)) = l((\bar{x} : \mathtt{Q} : \bar{y})) \geq l([\bar{x}, \bar{y}]) = d_{\mathcal{L}}(\bar{x}, \bar{y})$.

To show that ">" of the inequality holds for at least one pair x, y and thus the discrete CAT(0) inequality is violated, let $(p : \mathtt{aa} : q)$ be the edge of the lattice (not necessarily part of the circumference of the triangle) where the additional vertex was introduced

(comparison edge $(\bar{p} : \mathtt{a} : \bar{q})$). Define x, y on the circumference of Δ by extending this edge to their geodesic segment $[x, y] = (x : \mathtt{aaa}... : p) \cdot (p : \mathtt{aa} : q) \cdot (q : \mathtt{aa}... : y) = (x : \mathtt{a}^n : y)$. The comparison segment is by construction of the additional vertex $[\bar{x}, \bar{y}] = (\bar{x} : \mathtt{aaa}... : \bar{p}) \cdot (\bar{p} : \mathtt{a} : \bar{q}) \cdot (\bar{q} : \mathtt{aa}... : \bar{y}) = (\bar{x} : \mathtt{a}^{n-1} : \bar{y})$. Then $d_{\mathcal{D}}(x, y) = l([x, y]) = n > n - 1 = l([\bar{x}, \bar{y}]) = d_{\mathcal{L}}(\bar{x}, \bar{y})$. □

Lemma 3.27. *Consider an even geodesic triangle Δ in a square lattice with defects $\mathcal{D}$ such that Δ encloses exactly one vertex defect. If this is a negative vertex defect, Δ satisfies the discrete* CAT(0) *inequality.*

Proof. Let $\bar{\Delta}$ in the square lattice $\mathcal{L}$ be a comparison triangle for Δ in $\mathcal{D}$. Let x, y be vertices on Δ and $[x, y]$ denote the geodesic segment between them. The comparison vertices are $\bar{x}, \bar{y}$ and are joined by the geodesic segment $[\bar{x}, \bar{y}]$. Let $(x : \mathtt{P} : y)$ be the path obtained from $[\bar{x}, \bar{y}]$ by going from $\mathcal{L}$ to $\mathcal{D}$, i.e. by removing a vertex.

If this vertex did lie on $[\bar{x}, \bar{y}]$, its (previously minimal) length gets decreased further and thus $(x : \mathtt{P} : y) = [x, y]$, i.e. $d_{\mathcal{D}}(x, y) = l([x, y]) \leq l([\bar{x}, \bar{y}]) = d_{\mathcal{L}}(\bar{x}, \bar{y})$ holds.

Now assume the vertex to be removed from another path $(\bar{x} : \mathtt{Q} : \bar{y}) \neq [\bar{x}, \bar{y}]$. If the resulting path $(x : \mathtt{Q} : y)$ still is longer than $(x : \mathtt{P} : y)$, this has no influence on the geodesic segment, i.e. $(x : \mathtt{P} : y) = [x, y]$ and $d_{\mathcal{D}}(x, y) = l([x, y]) = l([\bar{x}, \bar{y}]) = d_{\mathcal{L}}(\bar{x}, \bar{y})$.

On the other hand, if $l((x : \mathtt{P} : y)) > l((x : \mathtt{Q} : y))$ and $(x : \mathtt{Q} : y)$ has minimal length, i.e. $(x : \mathtt{Q} : y) = [x, y]$, then $d_{\mathcal{D}}(x, y) = l([x, y]) = l((x : \mathtt{Q} : y)) < l((x : \mathtt{P} : y)) = l([\bar{x}, \bar{y}]) = d_{\mathcal{L}}(\bar{x}, \bar{y})$. □

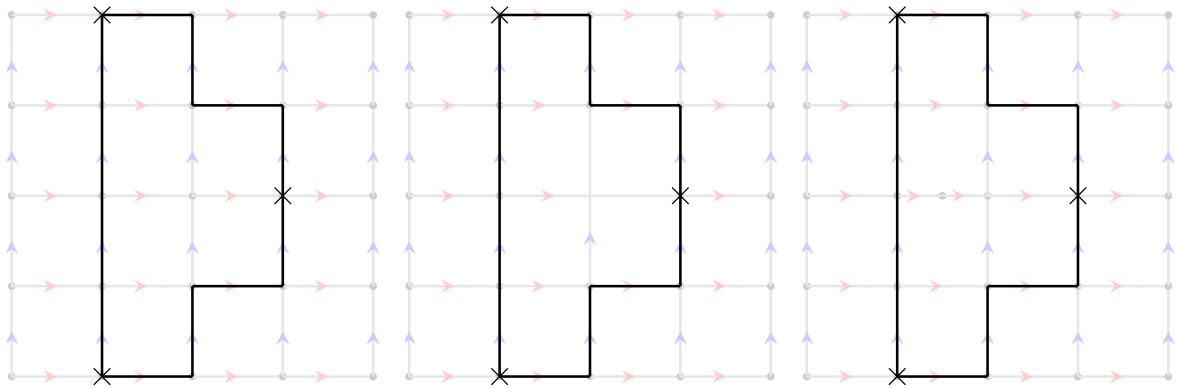

Figure 20: Geodesic triangles in lattices without defects (left), with negative (middle) and positive (right) vertex defect.

Corollary 3.28. *Consider an lattice geodesic triangle Δ in a square lattice with defects $\mathcal{D}$ such that Δ encloses exactly one vertex defect. Then this vertex defect is negative if and only if Δ satisfies the discrete* CAT(0) *inequality.*

Theorem 3.29. *Let $\mathcal{D}$ be a square lattice with defects. Then $\mathcal{D}$ fulfills the discrete* CAT(0) *inequality if and only if all vertex defects are negative.*

Proof. Consider $\mathcal{D}$ a square lattice with defects. If $\mathcal{D}$ does not contain any vertex defects, $\mathcal{D} = \mathcal{L}$ for $\mathcal{L}$ a square lattice and the equivalence holds trivially. Otherwise, consider a square lattice $\mathcal{L}$ with cardinals denoted by $\mathtt{a}$ and $\mathtt{b}$ for comparison.

Now let $\mathcal{D}$ contain at least one vertex defect. For the first implication, let $\mathcal{D}$ be CAT(0). Consider a vertex defect in $\mathcal{D}$ and denote $(\bar{x} : \mathtt{aa} : \bar{y})$ a path of $\mathcal{L}$ where the defect was introduced. Then define the path $c = (\bar{x} : \mathtt{baab^*b^*a^*a^*b} : \bar{x})$ in $\mathcal{L}$ and vertices $\bar{q}, \bar{r}$ on c that are the endpoints of the geodesic segments $[\bar{x}, \bar{q}] = (\bar{x} : \mathtt{b} : \bar{q})$ and $[\bar{x}, \bar{r}] = (\bar{x} : \mathtt{b^*aa} : \bar{r})$. This gives a geodesic triangle $\bar{\Delta}(\bar{x}, \bar{q}, \bar{r})$. Introducing the vertex defect and thus transforming $\mathcal{L}$ into $\mathcal{D}$ results in a lattice geodesic triangle Δ that encloses the vertex defect. Since $\mathcal{D}$ is CAT(0), by Corollary 3.28 the vertex defect is negative. By repeating this procedure for all defects of $\mathcal{D}$, one obtains that all defects must be negative.

For the reverse implication, let $\Delta = \Delta(p, q, r)$ be a lattice geodesic triangle in $\mathcal{D}$ and by hypothesis all vertex defects in $\mathcal{D}$ are negative. Let n be the number of vertex defects enclosed by Δ. Proof by induction:
$\underline{n = 0}$ If Δ does not enclose a vertex defect, it satisfies the discrete CAT(0) inequality trivially.
$\underline{n = 1}$ If Δ encloses exactly one vertex defect, it fulfills the discrete CAT(0) inequality due to Corollary 3.28.
$\underline{n \to n+1}$ If Δ encloses $n+1$ vertex defects, consider cardinals $\mathtt{a}_x, \mathtt{a}_y \in \{\mathtt{a}, \mathtt{b}\}$ such that $e_x = (\bar{x}_1 : \mathtt{a}_x\mathtt{a}_x : \bar{x}_2)$ and $e_y = (\bar{y}_1 : \mathtt{a}_y\mathtt{a}_y : \bar{y}_2)$ are paths of $\mathcal{L}$ that are affected by introducing the defects for $\mathcal{D}$ and $e_x \neq e_y$. Consider $\bar{o}$ on a geodesic through x_i and y_j, $i, j \in \{1, 2\}$ such that $\bar{o}$ is not on the circumference of $\bar{\Delta}$. Then there exists a cardinal $\mathtt{a}_o$ such that e_x, e_y lie on opposite sides of the geodesic c_o through o defined by the pathword $\mathtt{a}_o^m$ for some $m \in \mathbb{N}$. Define $\bar{v} \neq \bar{w}$ in the circumference of $\bar{\Delta}$ by the paths $(\bar{v} : \mathtt{a}_o^k : \bar{o})$ and $(\bar{o} : \mathtt{a}_o^\ell : \bar{w})$ with $k, \ell \in \mathbb{N}$. Since these are geodesic segments $[\bar{v}, \bar{o}]$, $[\bar{o}, \bar{w}]$ (in particular, $[\bar{v}, \bar{o}] \cdot [\bar{o}, \bar{w}] = [\bar{v}, \bar{w}]$ is part of the geodesic c_o) and $\bar{o} \notin \bar{\Delta}$, not all of the three vertices of $\bar{\Delta}$ lie on the same side of c_o. Without loss of generality, p and q lie on opposite sides of c_o. Then consider the geodesic triangles $\bar{\Delta}^p = \bar{\Delta}(\bar{v}, \bar{w}, \bar{p})$ and $\bar{\Delta}^q = \bar{\Delta}(\bar{v}, \bar{w}, \bar{q})$ such that $\bar{r}$ lies on the circumference of one of these. Now transform $\mathcal{L}$ into $\mathcal{D}$ by introducing the vertex defects. By construction of $\bar{v}$ and $\bar{w}$, the triangles $\Delta^p = \Delta(v, w, p)$ and $\Delta^q = \Delta(v, w, q)$ enclose n or less vertex defects and thus by hypothesis the discrete CAT(0) inequality holds for both of them. To show that $\Delta(p, q, r)$ fulfills this inequality, choose $z, u \in \Delta \subseteq \Delta^p \cup \Delta^q$. If $z, u \in \Delta^p$ or $z, u \in \Delta^q$, the inequality $d_{\mathcal{D}}(z, u) \leq d_{\mathcal{L}}(\bar{z}, \bar{u})$ follows from the CAT(0) property of the respective triangle. If z and u lie on opposite sides of $[v, w]$, define $\bar{s} \in \bar{\Delta}^p \cap \bar{\Delta}^q$ to be the intersection point of $[\bar{z}, \bar{u}]$ and $[\bar{v}, \bar{w}]$. Then follows $d_{\mathcal{D}}(z, u) \leq d_{\mathcal{D}}(z, s) + d_{\mathcal{D}}(s, u) \leq d_{\mathcal{L}}(\bar{z}, \bar{s}) + d_{\mathcal{L}}(\bar{s}, \bar{u}) = d_{\mathcal{L}}(\bar{z}, \bar{u})$, thus Δ is CAT(0). □

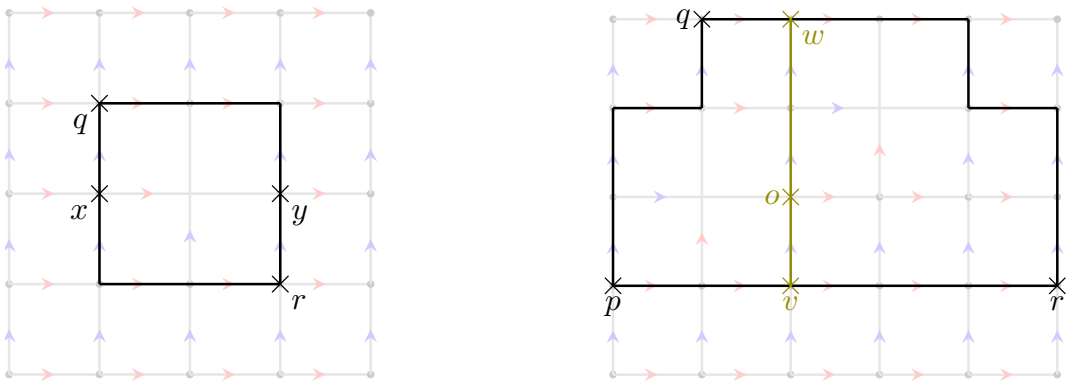

Figure 21: Setting for the first implication (left) and the induction in the second implication (right) of Theorem 3.29.

3.3 Arbitrary CAT(0) quivers

For arbitrary quivers, more than two cardinals might be defined. In this setting, it is not sensible to define lattice geodesic triangles as in Definition 3.15. Instead, this property is replaced by the weaker condition of even geodesic triangles:

Definition 3.30. *Consider a quiver $\mathcal{Q}$ and geodesic triangle Δ on it. If P_Δ is even and for all geodesic segments c_i that are sides of Δ the inequality $l(c_i) < \frac{P_\Delta}{2}$ holds, Δ is called an* even geodesic triangle.

Remark 3.31. All triangles on a square lattice $\mathcal{L}$ are even: Their circumference needs to be closed and on a square lattice with cardinals $\mathtt{x}$ and $\mathtt{y}$ this implies that $n_\mathtt{x} = n_{\mathtt{x}^*}$ and $n_\mathtt{y} = n_{\mathtt{y}^*}$ must hold. Therefore the length of any closed path is $n = 2(n_\mathtt{x} + n_\mathtt{y})$, i.e. even. Furthermore, a triangle Δ on a square lattice that has one side of length $\frac{P_\Delta}{2}$ is degenerate and if this value gets exceeded, it cannot be closed.

Lemma 3.32. *Consider a quiver $(\mathcal{Q}, d_\mathcal{Q})$ and $\Delta = \Delta(p, q, r)$ an even geodesic triangle in $\mathcal{Q}$. Then there exist vertices $\bar{p}, \bar{q}, \bar{r}$ in the square lattice $(\mathcal{L}, d_\mathcal{L})$ such that $d_\mathcal{Q}(p, q) = d_\mathcal{L}(\bar{p}, \bar{q})$, $d_\mathcal{Q}(q, r) = d_\mathcal{L}(\bar{q}, \bar{r})$, $d_\mathcal{Q}(r, p) = d_\mathcal{L}(\bar{r}, \bar{p})$.*

Definition 3.33. *For an even geodesic triangle Δ on $\mathcal{Q}$ and a triangle $\bar{\Delta} = \bar{\Delta}(\bar{p}, \bar{q}, \bar{r})$ in $\mathcal{L}$ that satisfies $d_\mathcal{Q}(p, q) = d_\mathcal{L}(\bar{p}, \bar{q})$, $d_\mathcal{Q}(q, r) = d_\mathcal{L}(\bar{q}, \bar{r})$, $d_\mathcal{Q}(r, p) = d_\mathcal{L}(\bar{r}, \bar{p})$, $\bar{\Delta}$ is called a* comparison triangle *for Δ.*

Proof. Fix a vertex $\bar{p}$ in $\mathcal{L}$ and denote the cardinals of $\mathcal{L}$ with $\mathtt{x}$ and $\mathtt{y}$. Define $n_\mathtt{x} = d_\mathcal{Q}(r, p)$ and $n = P_\Delta = d_\mathcal{Q}(p, q) + d_\mathcal{Q}(q, r) + d_\mathcal{Q}(r, p)$. The latter is even since Δ is even, thus $n_\mathtt{y} := \frac{d_\mathcal{Q}(p,q) + d_\mathcal{Q}(q,r) - d_\mathcal{Q}(r,p)}{2} = \frac{n - 2n_\mathtt{x}}{2} \in \mathbb{N}$. Furthermore, $d_\mathcal{Q}(p, q) \leq \frac{P_\Delta}{2} = \frac{n}{2}$ implies $d_\mathcal{Q}(q, r) = n - d_\mathcal{Q}(p, q) - n_\mathtt{x} > n - \frac{n}{2} - n_\mathtt{x} = n_\mathtt{y}$ and for $d_\mathcal{Q}(p, q)$ analogously. Define the vertices $\bar{r}, \bar{q}$ by the geodesic segments $[\bar{p}, \bar{r}] = (\bar{p} : \mathtt{x}^{n_\mathtt{x}} : \bar{r})$ and $[\bar{p}, \bar{q}] = (\bar{p} : \mathtt{y}^{n_\mathtt{y}} \mathtt{x}^{d_\mathcal{Q}(p,q) - n_\mathtt{y}} : \bar{q})$, respectively. The triangle can be closed by $[\bar{r}, \bar{q}] = (\bar{r} : \mathtt{y}^{n_\mathtt{y}} (\mathtt{x}^*)^{d_\mathcal{Q}(r,q) - n_\mathtt{y}} : \bar{q})$. These segments are indeed geodesic ones since they only contain either a cardinal or its inverse

and they have the appropriate lengths by construction. The concatenation is of length $n_{\mathtt{x}} + n_{\mathtt{y}} + d_{\mathcal{Q}}(p,q) - n_{\mathtt{y}} + n_{\mathtt{y}} + d_{\mathcal{Q}}(r,q) - n_{\mathtt{y}} = n$ and gives the circumference of $\bar{\Delta}$. □

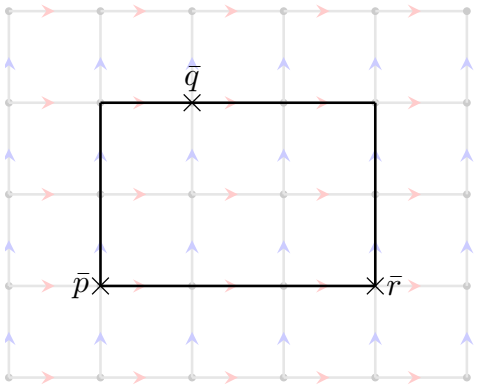

Figure 22: Example for a comparison triangle constructed as in the proof of Lemma 3.32. This is done by first fixing $\bar{p}$ and then constructing $[\bar{p}, \bar{r}]$ and $[\bar{p}, \bar{q}]$.

Definition 3.34. *Given an even geodesic triangle Δ in the quiver $(\mathcal{Q}, d_{\mathcal{Q}})$ and a comparison triangle $\bar{\Delta}$ in the square lattice $(\mathcal{L}, d_{\mathcal{L}})$, the tuple $(\Delta, \bar{\Delta})$ satisfies the* discrete CAT(0) inequality *if for all points $x, y \in \Delta$ and comparison points $\bar{x}, \bar{y} \in \bar{\Delta}$ holds the inequality:*

$$d_{\mathcal{Q}}(x,y) \leq d_{\mathcal{L}}(\bar{x}, \bar{y}) \tag{19}$$

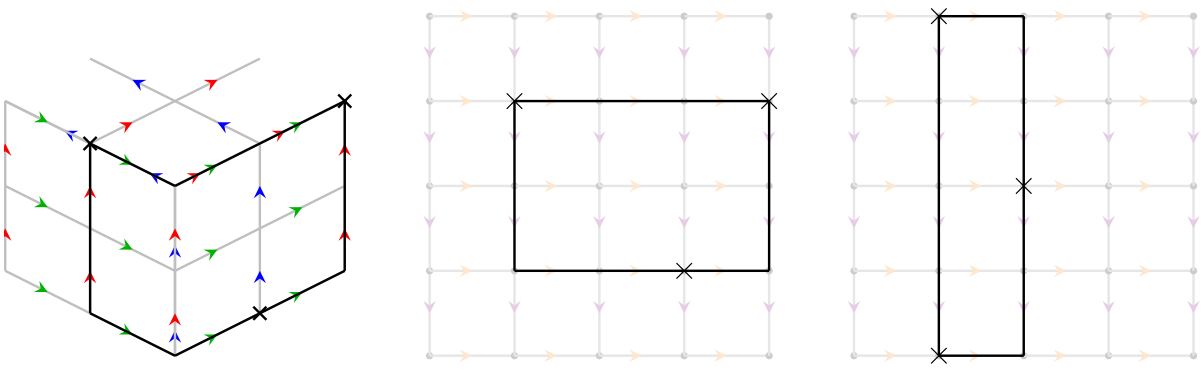

Figure 23: The procedure described in Lemma 3.32 does not yield unique triangles.

Remark 3.35. For triangles in arbitrary quivers with more than two cardinals, congruency is in general not uniquely defined. It is thus not sensible to talk about *the* comparison triangle for a geodesic triangle $\Delta \subseteq \mathcal{Q}$. Instead, both Δ and $\bar{\Delta}$ have to be specified beforehand and the CAT(0) property can only be defined given such a pair. However, this concept is not useful to compare arbitrary triangles in a quiver $\mathcal{Q}$ to "their" respective comparison triangles and infer statements about the curvature of $\mathcal{Q}$.

4 Cardinal charts and defects

The existence of comparison triangles for arbitrary quivers was shown in Lemma 3.32. However, the analysis of defects by comparison with a square lattice is more involved in this case. A simpler way to investigate it is to consider cardinal charts and chart defects as described in this section. Again, $\mathcal{Q}$ denotes a quiver.

4.1 Cardinal charts and atlases

In a square lattice, the two cardinals are defined at any vertex of the quiver. However, this is not the case in general. Instead, the concepts of charts and atlases are needed to describe it.

Definition 4.1. *For a quiver $\mathcal{Q}$ with vertex set V, a* connected subset *U is a subset of V such that for any $u, w \in U$ exists a path c from u to w in U.*

Definition 4.2. *Consider a quiver $\mathcal{Q}$ with cardinals $\mathtt{c}_1, ..., \mathtt{c}_n$ and a connected subset U. Then a* cardinal chart *of U is a choice of cardinals $C = (\mathtt{c}_{i_1}, ..., \mathtt{c}_{i_k})$ such that for each edge e between vertices in U exactly one cardinal that labels e is present in C. The connected subset U is called the* domain *of C and k is its* cardinality.

Remark 4.3. For simplicity, we abbreviate "cardinal charts" throughout this thesis but call them *charts* instead. However, they should not be confused with the concept of charts on manifolds.

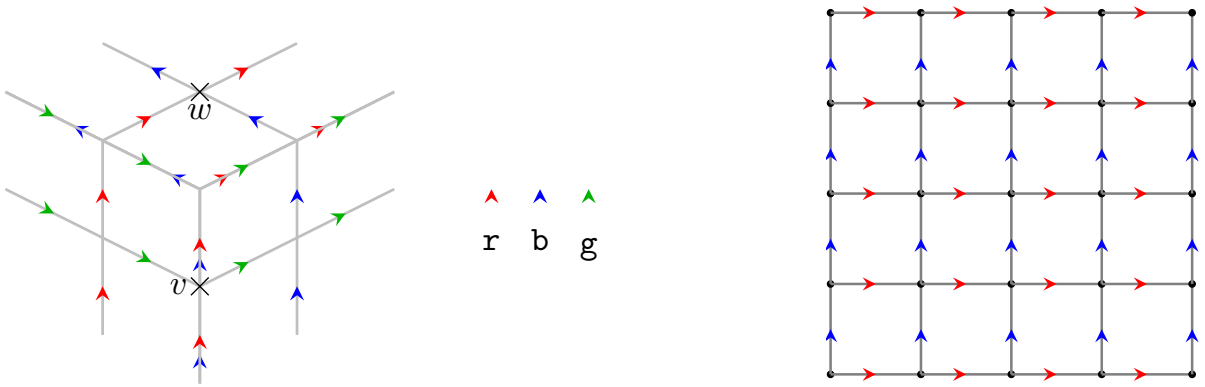

Figure 24: Quivers with different cardinals. In a neighbourhood of the vertex w in the left quiver, the same chart as on the square lattice on the right can be defined. The cardinals at the vertex v allow for different charts in a neighbourhood of this vertex.

Example 4.4. (i) In Fig. 24, in a neighbourhood of the vertex w in the left quiver (as well as in any subset of the square lattice) a possible chart is $(\mathtt{r}, \mathtt{b})$. Alternative charts are combinations with the inverse cardinals, i.e. $(\mathtt{r}^*, \mathtt{b})$, $(\mathtt{r}, \mathtt{b}^*)$ and $(\mathtt{r}^*, \mathtt{b}^*)$. In neighbourhoods of the vertex v, both $(\mathtt{g}, \mathtt{b})$ and $(\mathtt{g}, \mathtt{r})$ can be defined as well as

respective combinations with the inverse cardinals. In particular, different connected subsets of this quiver allow for different charts (Fig. 25).

(ii) Consider the quivers $\mathcal{L}, \mathcal{D}_-, \mathcal{D}_+$ (square lattice without, with negative and with positive defects, respectively) with cardinals $\mathtt{r}, \mathtt{b}$ given in Fig. 18 and denote V, V_-, V_+ their respective sets of vertices. In $\mathcal{D}_-$, a chart for V_- is given by $(\mathtt{r}, \mathtt{b})$. In contrary, the set $V_+ \setminus V \subseteq V_+$ (the set that contains only the additional vertex) defined on $\mathcal{D}_+$ has the chart $(\mathtt{r})$ while a chart for $V \subseteq V_+$ is $(\mathtt{r}, \mathtt{b})$.

(iii) With a chart fixed, we can also refer to the cardinals by their indices in the tuple. For example, with $C = (\mathtt{r}, \mathtt{b})$ in a square lattice $\mathcal{L}$ with vertices x, y, the path $c = (x : \mathtt{rbbr}^* : y)$ can be expressed as $c = (x : 1221^* : y)$.

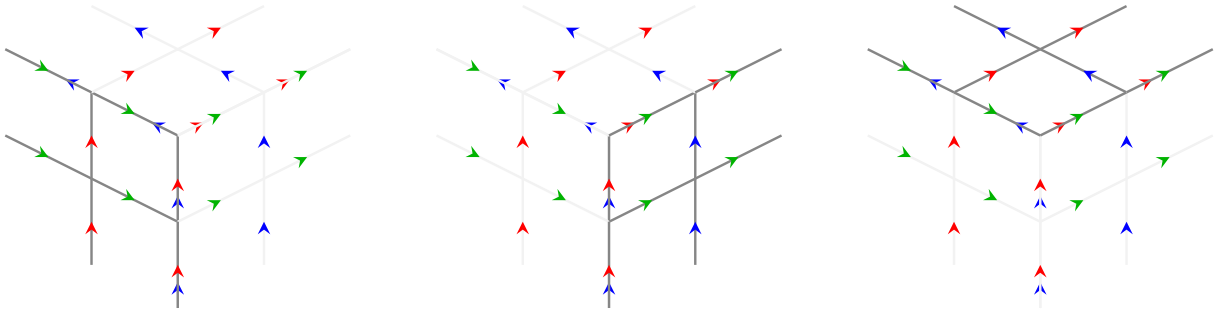

$(\mathtt{r}, \mathtt{g})$ $(\mathtt{g}, \mathtt{b})$ $(\mathtt{b}, \mathtt{r})$

Figure 25: For different connected subsets of the left quiver in Fig. 24, different charts can be defined.

Remark 4.5. The *set of charts of cardinality* k is denoted by Γ_k. The set Γ_{k-1} can be embedded into Γ_k by using the *blank cardinal* _ and the embedding $\iota : \Gamma_{k-1} \hookrightarrow \Gamma_k$, $(\mathtt{c}_1, ..., \mathtt{c}_{k-1}) \mapsto (\mathtt{c}_1, ..., \mathtt{c}_{k-1}, \_)$. The blank cardinal does not have a specified direction and thus it cannot be inverted.

To be able to change between charts, they have to overlap. This means that some edges must be labelled by more than one cardinal. Since these are equivalent descriptions of the same edge, they define a correspondence that can be used to change between charts.

Definition 4.6. *Consider charts* $C = (\mathtt{c}_1, ..., \mathtt{c}_k)$, $C' = (\mathtt{c}'_1, ..., \mathtt{c}'_k) \in \Gamma_k$ *with* U, U' *satisfying* $U \cap U' \neq \emptyset$ *and for all* $i = 1, ..., k$ *the cardinals* $\mathtt{c}_i, \mathtt{c}'_i$ *label the same edges in* $U \cap U'$. *Then the tuple* $\rho = (C, C')$ *is called a* transition. *The count of indices where* C *and* C' *differ is called the* dimension *of* ρ.

Example 4.7. On the quiver in Fig. 26, the charts $C = (\mathtt{g}, \mathtt{b})$ and $C' = (\mathtt{g}, \mathtt{r})$ can be defined. The transition (C, C') is given by the cardinal rewrite $\mathtt{b} \mapsto \mathtt{r}$.

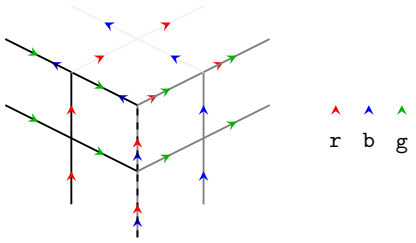

Figure 26: Setting to define a transition between $C = (\mathtt{g}, \mathtt{b})$ and $C' = (\mathtt{g}, \mathtt{r})$. The domains U and U' are marked in gray and black, respectively

Definition 4.8. *Given a transition $\rho = (C, C')$ with $C = (\mathtt{c}_1, ..., \mathtt{c}_k)$, $C' = (\mathtt{c}'_1, ..., \mathtt{c}'_k)$, the cardinals at the same position $i \in \{1, ..., k\}$ correspond to each other. These correspondences are called* cardinal rewrites *and are denoted by $\mathtt{c}_i \mapsto \mathtt{c}'_i$. In this way, ρ can be identified with the set of cardinal rewrites $\tilde{R}_\rho = \{\mathtt{c}_1 \mapsto \mathtt{c}'_1, ..., \mathtt{c}_k \mapsto \mathtt{c}'_k\}$ which in turn is equivalent to the subset of non-trivial cardinal rewrites $R_\rho = \{(\mathtt{a} \mapsto \mathtt{b}) \in \tilde{R}_\rho \mid \mathtt{a} \neq \mathtt{b}\}$. The latter is called* chart rewrite *and it contains $d = \dim(\rho) = |R_\rho|$ cardinal rewrites.*

Remark 4.9. For any chart $C = (\mathtt{c}_1, ..., \mathtt{c}_k)$ with domain U exists the chart $C_{\mathtt{c}_i^*} = (\mathtt{c}_1, ..., \mathtt{c}_i^*, ..., \mathtt{c}_k)$ with the same domain U such that the transition $(C, C_{\mathtt{c}_i^*})$ has chart rewrite $\{\mathtt{c}_i \mapsto \mathtt{c}_i^*\}$. A transition with a chart rewrite that contains only cardinal rewrites from a cardinal to its inverse is called a *inverting transition.*

Furthermore, given any two charts C, C' on a quiver $\mathcal{Q}$ with domains U, U' such that $U \cap U'$ contains at least two vertices v, w with $d(v, w) = 1$, exists a transition (C, C').

Definition 4.10. *Consider a set A of charts $C_i, i \in I$ on $\mathcal{Q}$ with domains $U_i, i \in I$ for some index set I such that the following two properties hold:*

(i) for all vertices $x \in \mathcal{Q}$ exists at least one $j \in I$ such that $U_j \ni x$

(ii) for all $U_i \in A$ exists $k \in I$ and $v, w \in U_i \cap U_k$ with $d(v, w) = 1$

Then A is an atlas *of the quiver $\mathcal{Q}$.*

Definition 4.11. *Let $\mathcal{Q}$ be a quiver with vertex set V, $x, y \in V$ and $c = (x : \mathtt{P} : y)$ be a path in $\mathcal{Q}$. Given an atlas A of $\mathcal{Q}$, define a* cardinal transport *from C_0 to C_k to be $\tau = (\rho_i)_{i \in \{1,...,k\}} = ((C_{i-1}, C_i))_{i \in \{1,...,k\}}$. It is given by the sequence of transitions that are needed along the path c to transform the chart C_0 defined at x to a chart C_k defined at y. The set of charts associated to this cardinal transport gives the* chart path *$\Gamma_\tau = \{C_i \mid i \in \{0, ..., k\}\} \subseteq A$. By the transitions ρ_i being equivalent to chart rewrites R_i, the* path rewrite *$R_\tau = \bigcup_{i=1}^{k} R_i$ is associated to the cardinal transport τ.*

Remark 4.12. Cardinal transport along a path is not necessarily unique. Since each cardinal transport has an associated chart path and path rewrite, there might be different chart paths and path rewrites along one path in the quiver.

In general, a cardinal transport cannot be described equivalently by the associated path rewrite, since the path rewrite does not preserve the order of the transitions.

Example 4.13. Consider the quiver in Fig. 27 and the path $c = (x : \mathtt{gg} : y)$. For a cardinal transport, consider the chart $C_x = (\mathtt{g}, \mathtt{r})$. After following c to the vertex v, this has to be changed by the cardinal rewrite $\mathtt{b} \mapsto \mathtt{r}$, since C_x is not defined at the next vertex (y). In this way, C_x is transformed to $C_y = (\mathtt{g}, \mathtt{r})$. The transition is $\rho = (C_x, C_y)$ and the cardinal transport $\tau = \{\rho\}$. Since only one transition is needed, the chart rewrite an the path rewrite are the same, $R_\rho = \{\mathtt{b} \mapsto \mathtt{r}\} = R_\tau$.

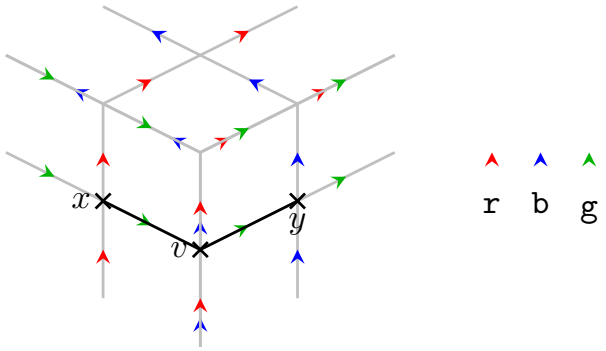

Figure 27: Setting to define cardinal transport from x to y.

4.2 Chart defects

In order to analyse defects with the help of charts, we need to consider certain sets of vertices and the charts defined for these. Consider A an atlas of $\mathcal{Q}$.

Definition 4.14. *For a connected subset U, a* sub-atlas $A_U \subseteq A$ *is a set of charts such that for every vertex $u \in U$ exists at least one chart $C \in A_U$ with domain U_C with $u \in U_C$.*

Definition 4.15. *Given two cardinal rewrites $\mathtt{a} \mapsto \mathtt{b}$, $\mathtt{b} \mapsto \mathtt{c}$, they can be applied transitively to obtain a new rewrite by the* composition $(\mathtt{b} \mapsto \mathtt{c}) \circ (\mathtt{a} \mapsto \mathtt{b}) = (\mathtt{a} \mapsto \mathtt{c})$.

Definition 4.16. *A cardinal transport τ from C_x to $\tilde{C}_x$ as defined in Definition 4.11 along a closed path $c = (x : \mathtt{P} : x)$ is said to be* inconsistent *if it does not contain any inverting transitions (Remark 4.9) and there exist a cardinal $\mathtt{a}$ and rewrites in the path rewrite R_τ with composition $\mathtt{a} \mapsto \mathtt{a}^*$.*

Definition 4.17. *Let U be a connected subset of $\mathcal{Q}$ with sub-atlas $A_U \subseteq A$. Then A_U is said to be* inconsistent *if there exists a closed path $c = (x : \mathtt{P} : x)$ in U and a cardinal transport τ along c that is inconsistent in the sense of Definition 4.16. In this case, U is said to harbour a* chart defect.

Example 4.18. Consider the quivers and paths in Fig. 28.

(i) Cardinal transport along $x : \mathtt{rrb}^*\mathtt{b}^*\mathtt{g}^*\mathtt{g}^* : x$ changes the chart $C_x = (\mathtt{g}, \mathtt{r})$ to $C_w = (\mathtt{b}^*, \mathtt{r})$, then to $C_y = (\mathtt{b}^*, \mathtt{g})$ and $C'_x = (\mathtt{r}^*, \mathtt{g})$. This gives the path rewrite $R = \{\mathtt{g} \mapsto \mathtt{b}^*, \mathtt{r} \mapsto \mathtt{g}, \mathtt{b}^* \mapsto \mathtt{r}^*\}$. The composition of $\mathtt{r} \mapsto \mathtt{g}$, $\mathtt{g} \mapsto \mathtt{b}^*$ and $\mathtt{b}^* \mapsto \mathtt{r}^*$ yields $\mathtt{r} \mapsto \mathtt{r}^*$ which indicates the presence of a chart defect.

(ii) The path $d = (o : \texttt{rrrbr}^*\texttt{r}^*\texttt{b}^* : o)$ induces a cardinal transport changing from $C_o = (\texttt{r}, \texttt{b})$ to $C_p = (\texttt{r}, \_)$, where $\_$ indicates the missing cardinal at p, then to $C_q = (\texttt{r}, \texttt{b}^*)$ and back to C_o. Since $\texttt{b} \mapsto \_$ (by the transition $\rho_0 = (C_o, C_p)$) and $\_ \mapsto \texttt{b}^*$ (by $\rho_1 = (C_p, C_q)$), yield the composition $\texttt{b} \mapsto \texttt{b}^*$, a chart defect must be present.

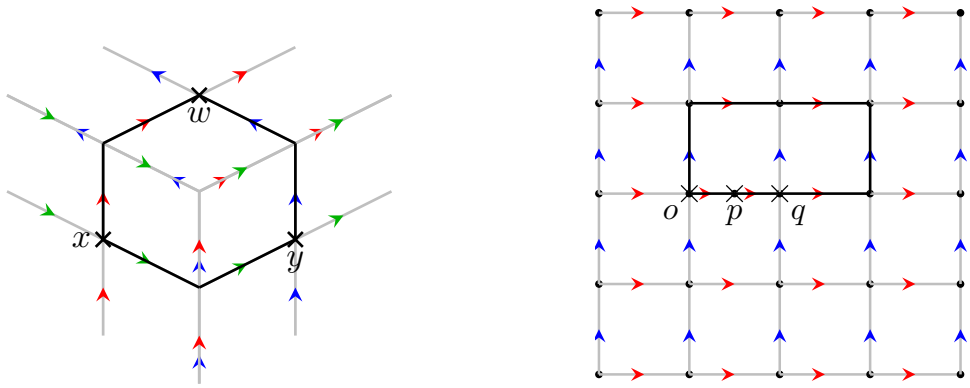

(i) (ii)

Figure 28: Examples of inconsistent cardinal transports. The numbering corresponds to the one in Example 4.18.

Remark 4.19. A sub-atlas that is not inconsistent in the sense of Definition 4.17 is a consistent sub-atlas. The maximal dimension of a transition between two charts in a consistent sub-atlas T gives its *dimension* $\dim(T) = \max_{C,C' \in T} \dim((C, C'))$. Any sub-atlas that contains only one chart is a 0-dimensional consistent sub-atlas by construction.

Lemma 4.20. *Let $\mathcal{D}$ be a square lattice with defects. $\mathcal{D}$ does contain at least one chart defect if and only if it contains any positive vertex defect.*

Proof. For $\mathcal{D}$ a square lattice with defects, consider the following cases: If $\mathcal{D}$ contains a positive vertex defect, the additional vertex introduced at the vertex defect has a chart that contains one cardinal only. In this case, an inconsistent cardinal transport can be constructed as in (ii) of Example 4.18, i.e. $\mathcal{D}$ contains a chart defect. On the other hand, if $\mathcal{D}$ does not harbour any positive vertex defect, all vertices have the same chart (e.g. $(\texttt{r}, \texttt{b})$ in the case of the left quiver in Fig. 18) and thus no chart defect is present. □

Theorem 4.21. *A square lattice with defects $\mathcal{D}$ is* CAT(0) *if and only if it does not harbour any chart defect.*

Proof. By Theorem 3.29, for a square lattice with defects not being CAT(0) is equivalent to having any positive defect, which in turn is, by Lemma 4.20, is the case if and only if a chart defect is present. □

5 CAT(0) cube complexes

Another example of metric spaces that can be investigated with the help of CAT(0) geometry are cube complexes. The following concepts are based on [BH99] and [Sch19] and will be needed to state and prove Gromov's link condition.

5.1 Construction

Definition 5.1. *Given $n \in \mathbb{N}_0$, define the* n-cube C^n *to be a point if $n = 0$ and $C^n = [0,1]^n$ otherwise. It is isometric to a (filled) cube in Euclidean space $\mathbb{R}^n$ and n is called its* dimension.[1]

Definition 5.2. *For an n-cube C^n, a* face F *of C^n is given by $F = F_1 \times ... \times F_n$ where $F_i \in \{\{0\}, \{1\}, [0,1]\}$. The latter set is the set of faces of the 1-cube $[0,1]$. The* dimension *of a face F is $\dim F = \sum_{i=1}^{n} \dim F_i$.*

Definition 5.3. *Given $n \geq 1$, $\epsilon > 0$ and a cube $C^{n+1} \cong [0,1]^{n+1}$ endowed with the metric d_{C^n}, consider v a vertex of C^{n+1} and $F_i^{C^{n+1}}$ faces of C^{n+1}. Then, $S^n = \{x \in C^{n+1} \mid d_{C^n}(v,x) = \epsilon\}$ is the* all-right spherical shape *of dimension n. Its* faces *are given by $F_i^S = F_i \cap S^n$ and the* metric d_{S^n} *on S^n is defined by the Euclidean angle at v in C^n, i.e. $d_{S^n}(p,q) = \angle_v(\bar{vp}, \bar{vq})$ for any $p, q \in S^n$.*

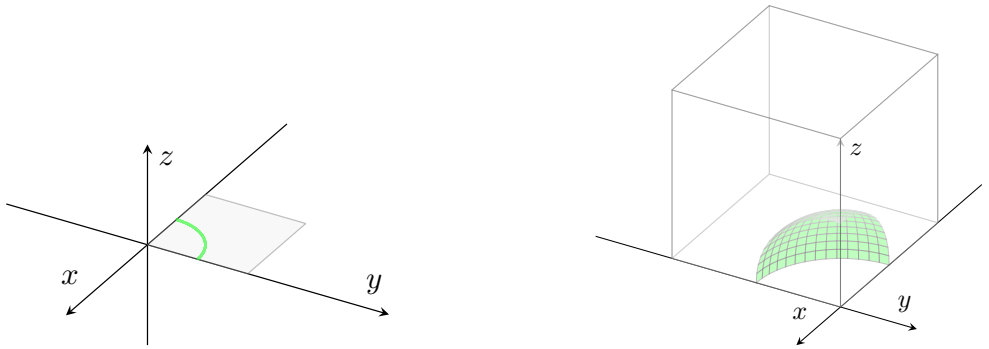

Figure 29: Examples of all-right spherical shapes (marked in green) of dimension $n = 1$ (left) and $n = 2$ (right).

Definition 5.4. *Consider two shapes (e.g. cubes or all-right spherical shapes) A and $\tilde{A}$ (of potentially different dimensions) and two faces $F, \tilde{F}$ of the respective shapes, $F \subseteq A$ and $\tilde{F} \subseteq \tilde{A}$. Then a* gluing *of A and $\tilde{A}$ is given by an isometry $\phi : F \to \tilde{F}$.*

Remark 5.5. Only shapes of the same kind can be glued together in the way given by Definition 5.4.

[1] Be aware that C^n with exponent refers to a cube while other C are denoting charts. However, cubes are only needed in this subsection (Section 5.1) to define cube complexes and will not be used afterwards.

Definition 5.6. *Let $\mathfrak{A}$ be a set of disjoint shapes of the same kind. Furthermore consider $\mathfrak{G}$ a set of gluings of pairwise different $A \in \mathfrak{A}$, i.e. no A is glued to itself, such that all pairs $A \neq \tilde{A} \in \mathfrak{A}$ are glued together by no more than one gluing. For $x, y \in \bigsqcup_{A\in\mathfrak{A}} A$ define the equivalence relation $\sim$ by*

$$x \sim y \Leftrightarrow \exists \text{ faces } F_x \ni x,\ F_y \ni y \text{ and a gluing } \phi \in \mathfrak{G}, \phi : F_x \to F_y \text{ such that } y = \phi(x) \tag{20}$$

*then $\mathbf{K}_{\mathfrak{A}} = \left(\bigsqcup_{A\in\mathfrak{A}} A\right)/\!\sim$ gives the A-*complex $\mathbf{K}_{\mathfrak{A}}$ *of dimension $n = \sup_{A\in\mathfrak{A}}(\dim(A))$.*

Definition 5.7. *Given a shape $A \in \mathfrak{A}$ and denoting the zero-dimensional faces by V_A and F_A the faces of A, then the quotient $V_{\mathfrak{A}} = \left(\bigsqcup_{A\in\mathfrak{A}} V_A\right)/\!\sim$ is called the set of* vertices of $\mathbf{K}_{\mathfrak{A}}$ *and $F_{\mathfrak{A}} = \left(\bigsqcup_{A\in\mathfrak{A}} F_A\right)/\!\sim$ the* faces of $\mathbf{K}_{\mathfrak{A}}$.

For $\mathfrak{A} = \mathfrak{C}$ a set of cubes, the resulting $\mathbf{K}_{\mathfrak{C}}$ is a cube complex. *Choosing $\mathfrak{A} = \mathfrak{S}$ a set of all-right spherical shapes results in $\mathbf{K}_{\mathfrak{S}}$ being an* all-right spherical complex.

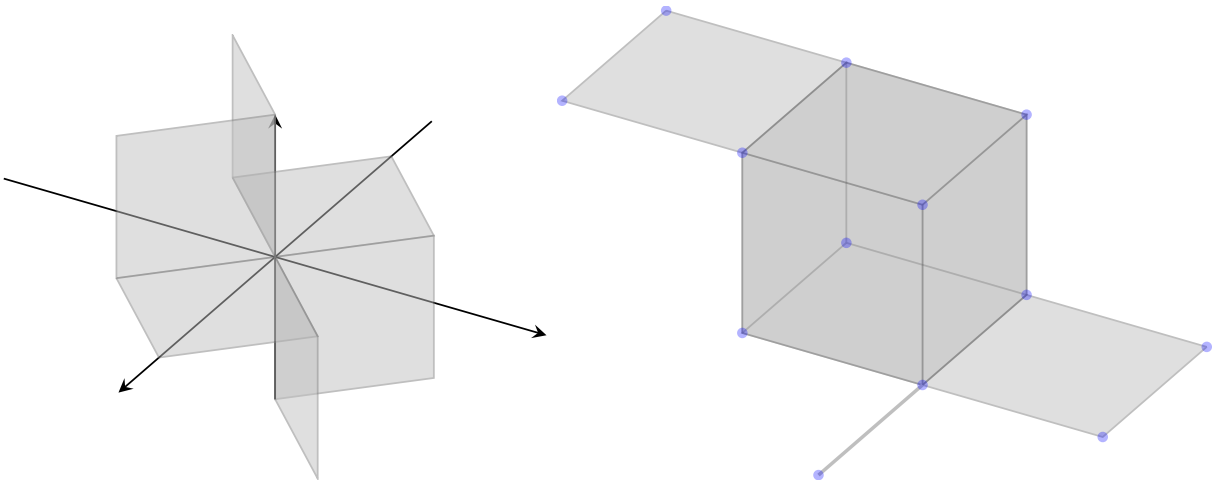

Figure 30: Examples of cube complexes of dimension $n = 2$ (left) and $n = 3$ (right). In the right complex, the vertices are marked in blue.

Definition 5.8. *Given a non-empty set V and a set $\mathfrak{A}$ of non-empty finite subsets of V, $\mathfrak{V} = (V, \mathfrak{A})$ is called an* abstract simplicial complex *if it fulfills the following properties:*

(i) $\{v\} \in \mathfrak{A}$ *for all* $v \in V$

(ii) If $A \in \mathfrak{A}$ then for all non-empty subsets $F \subseteq A$ holds $F \in \mathfrak{A}$.

V is the set of vertices *of $\mathfrak{V}$ and the elements of $\mathfrak{A}$ are its* simplices. *A simplex $A \in \mathfrak{A}$ with cardinality $n+1$ is called an n-*simplex *or simplex of dimension n. The elements of A are the* vertices *of the simplex and the non-empty subsets of A are its* faces.

Remark 5.9. In the setting and notation of Definition 5.6, the all-right spherical complex $\mathbf{K}_{\mathfrak{S}}$ is a geometric realisation of the abstract simplicial complex $(V_{\mathfrak{S}}, \mathfrak{S})$.

In general, cubical complex are no geometric realisations of abstract simplicial complexes. For example, given $\mathbf{K}_{\mathfrak{C}} = [0,1]^2 = C^2$ build from $V_{\mathfrak{C}} = \{(0,0),(0,1),(1,0),(1,1)\}$ and $\mathfrak{C}$ the set of C^2 and its faces, $(V_{\mathfrak{C}}, \mathfrak{C})$ is not an abstract simplicial complex since Definition 5.8 would require a subset of C^2 build of only three faces to be in $\mathfrak{C}$, too.

Definition 5.10. *Consider a set of metric spaces $\mathfrak{A} = \{(A_j, d_j) \mid j \in J\}$ for some index set J and the A-complex $\mathbf{K}$ given by Definition 5.6. Then the length of a continuous path $c : [0,1] \to \mathbf{K}$ is given by $l(c) = \sup_{x_i,\dots,x_n \in c([0,1])} \sum_{i=1}^{n-1} d_{j_i}(x_i, x_{i+1})$ where $x_i, x_{i+1} \in A_{j_i}$. In particular, for a sufficiently fine partition $\{x_1, \dots, x_n\}$ of $c([0,1])$ such j_i can be found for all $i = 1, \dots, n$. Since $\sum_{i=1}^{n-1} d_{j_i}(x_i, x_{i+1})$ increases with n, the supremum and thus the length of c is well-defined.*

Definition 5.11. *For an A-complex $\mathbf{K}$ constructed from a set of metric spaces $\mathfrak{A} = \{(A_j, d_j) \mid j \in J\}$ with index set J, define the* metric on $\mathbf{K}$ *in the following way: For $x, y \in \mathbf{K}$ let $d_{\mathbf{K}}(x,y) = \inf_{c \text{ path from } x \text{ to } y} l(c)$. If x, y lie in the same A_j, then $d_{\mathbf{K}}(x,y) = d_j(x,y)$.*

Remark 5.12. If we want to highlight the metric defined on a A-complex $\mathbf{K}$, we write $(\mathbf{K}, d_{\mathbf{K}})$. If not specified further, this metric is the one constructed in Definition 5.11.

Definition 5.13. *Consider an A-complex $(\mathbf{K}, d_{\mathbf{K}})$ and $v \in \mathbf{K}$ a vertex and fix $1 > \epsilon > 0$. The* link of v in $\mathbf{K}$ *is given by $\mathrm{Lk}(v, \mathbf{K}) = \{x \in \mathbf{K} \mid d_{\mathbf{K}}(v,x) = \epsilon\}$. This is an all-right spherical complex by construction. The metric d_{Lk} is defined analogously to the one in Definition 5.11 for all-right spherical complexes.*

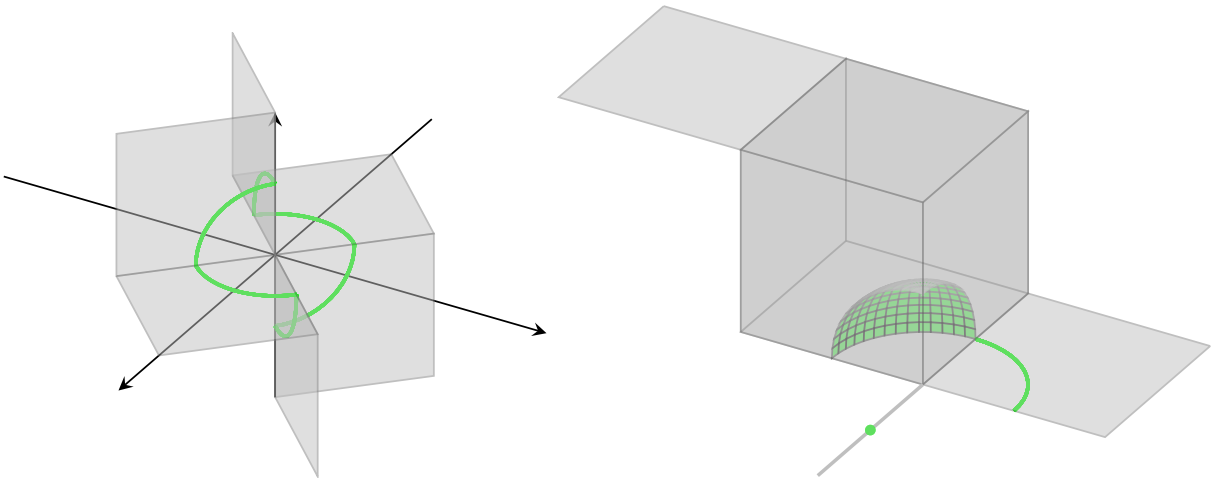

Figure 31: Link of the cube complexes given in Fig. 30.

Remark 5.14. Let $(\mathbf{K}, d_{\mathbf{K}})$ an A-complex and $v \in \mathbf{K}$ a vertex. The link $\mathrm{Lk}(v, \mathbf{K}) = \{x \in \mathbf{K} \mid d_{\mathbf{K}}(v,x) = \epsilon\}$ defined in Definition 5.13 for some $\epsilon \in (0,1)$ is independent of this ϵ up

to isometry. This can be seen similar to an n-sphere $\mathbb{S}^n(r) = \{x \in \mathbb{R}^{n+1} \mid |x| = r\}$ with radius r (equipped with the metric given by the Euclidean angle at the origin in $\mathbb{R}^{n+1}$) being isometric to any other n-sphere with different radius. For simplicity, we will embed $\mathrm{Lk}(v, \mathbf{K})$ into $\mathbf{K}$ by using unit vectors.

Abstractly, the link can be seen as the directions at v: Defining geodesic segments $[v, x], [v, y] \subseteq \mathbf{K}$ to be equivalent if one of them contains the other gives an equivalence relation $\approx$ on the set $\mathfrak{D}_v$ of geodesic segments starting at v such that $\mathfrak{D}_{v/\approx} \cong \mathrm{Lk}(v, \mathbf{K})$.

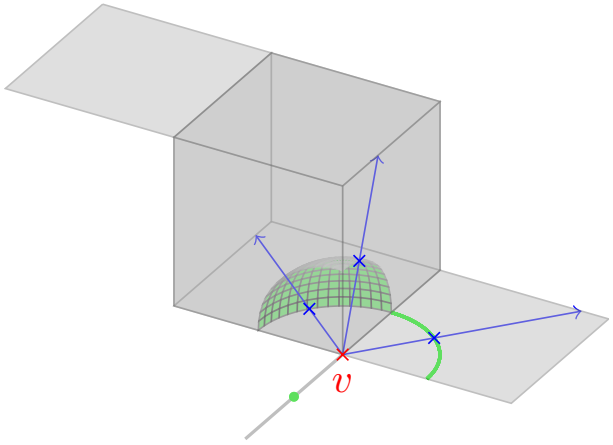

Figure 32: The link complex can be seen as the set of possible directions (blue lines) at a vertex v or as embedded into the cube complex (green object).

Definition 5.15. *Consider an abstract simplicial complex $(\mathfrak{S}, V_\mathfrak{S})$ as in Definition 5.8. A subset $\{v_0, ..., v_k\} \subseteq V_\mathfrak{S}$ for which $\{v_i, v_j\} \subseteq \{v_0, ..., v_k\}$ is a simplex for all $i, j \in \{0, ..., k\}$ is called a* k-skeleton.

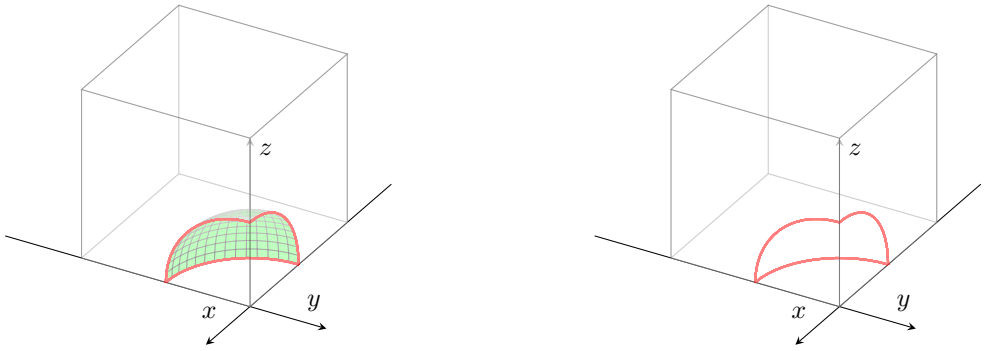

Figure 33: An all-right spherical simplex (left) and its skeleton only (right).

Definition 5.16. *An abstract simplicial complex $(\mathfrak{S}, V_\mathfrak{S})$ is a* flag complex *if all k-skeletons are k-simplices, i.e. if*

$$\{v_i, v_j\} \subseteq \{v_0, ..., v_k\} \subseteq V_\mathfrak{S} \text{ simplex } \forall i, j \in \{0, ..., k\} \Rightarrow \{v_0, ..., v_k\} \text{ simplex} \tag{21}$$

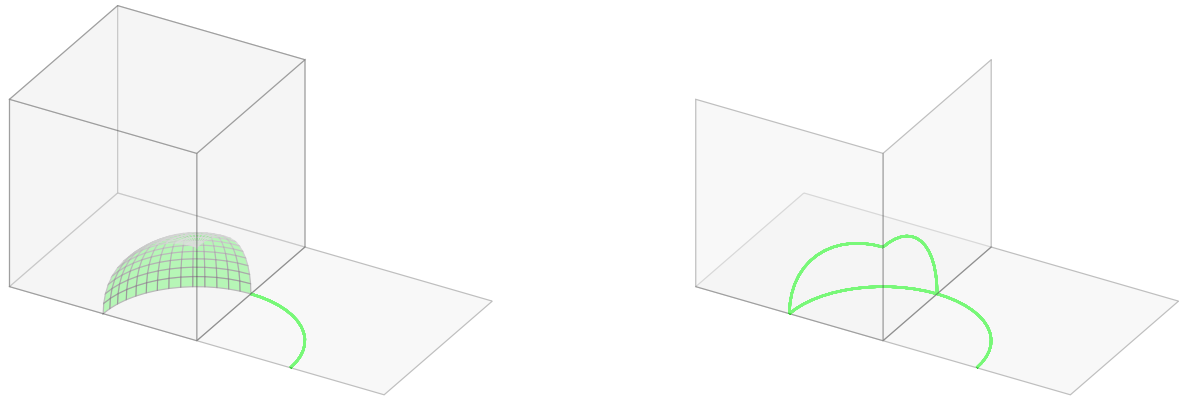

Figure 34: Examples for all-right spherical complexes being flag (left) and and failing the flag condition (right).

5.2 Gromov's link condition

With these definitions, we can state the central theorem of this thesis [Gro87]:

Theorem 5.17 (Gromov's link condition)**.** *Let* $\mathbf{K}$ *be a finite dimensional cube complex. Then* $\mathbf{K}$ *has curvature* ≤ 0 *if and only if for all* v *vertices of* $\mathbf{K}$ *the link* $\mathrm{Lk}(v, \mathbf{K})$ *is flag.*

The proof uses characterisations of the link complex being CAT(1), in particular the equivalence of CAT(1) and flag on the one hand and the connection of curvature and the link being CAT(1) on the other hand. The latter is stated in a general form by [BH99]:

Theorem 5.18. *A complex* $\mathbf{K}$ *with finitely many faces build from shapes* $A \subseteq M^n_\kappa, \kappa \in \mathbb{R}$ *has curvature* $\leq \kappa$ *if and only if for all vertices* v *the link* $\mathrm{Lk}(v, \mathbf{K})$ *is* CAT(1)*.*

In this thesis, we will show this for $\kappa = 0$ (Theorem 5.25) and $\kappa = 1$ (Lemma 5.19) only. The latter case together with Lemma 5.20 can then be used to prove the equivalence of CAT(1) and the condition to be flag (Lemmas 5.21 and 5.22) following [Sch19] and [DM99].

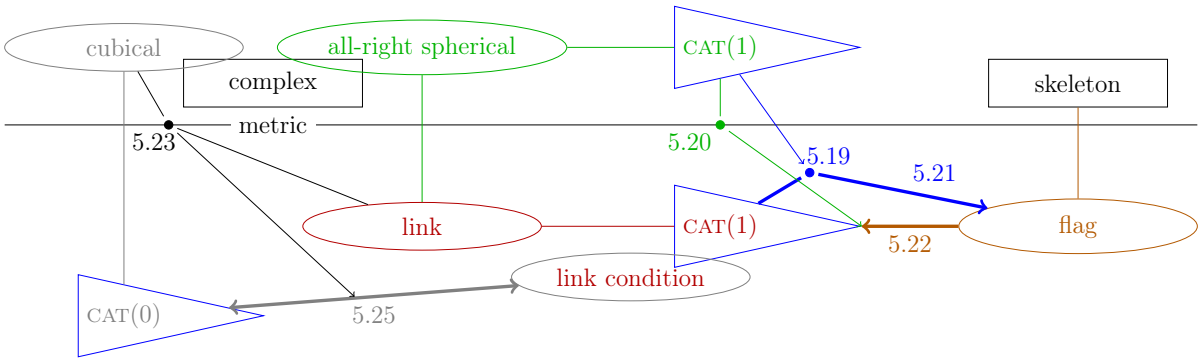

Figure 35: Overview of Section 5. The thick arrows give the implications used to proove Theorem 5.17.

Lemma 5.19. *Let* $\mathbf{L}$ *be a* CAT(1) *all-right spherical complex of finite dimension and* v *a vertex of* $\mathbf{L}$*. Then* $\mathrm{Lk}(v, \mathbf{L})$ *is* CAT(1)*.*

Proof. Consider $\mathbf{L}$ as stated and v a vertex in $\mathbf{L}$. Let $\Delta = \Delta(x, y, z) \subseteq \mathrm{Lk}(v, \mathbf{L})$ be a geodesic triangle. By construction of the link from $\mathbf{L}$, x, y, z can be embedded in $\mathbf{L}$. Denote these embeddings by $\tilde{x}, \tilde{y}, \tilde{z}$. They define a geodesic triangle $\tilde{\Delta} = \tilde{\Delta}(\tilde{x}, \tilde{y}, \tilde{z}) \subseteq \mathbf{L}$. In particular, under the metric $d_{\mathbf{L}}$ defined by the angles (Definition 5.3), geodesics obey the following: For $p, q \in \mathbf{L}$ with $d_{\mathbf{L}}(v, p) = d_{\mathbf{L}}(v, q)$ the points on the geodesic segment $[p, q]$ have the same distance to v as p and q. Thus, the geodesic segment $[\tilde{x}, \tilde{y}]$ is the same as the embedding of $[x, y]$ and in particular $d_{\mathrm{Lk}}(x, y) = d_{\mathbf{L}}(\tilde{x}, \tilde{y})$. The same holds for the other sides of Δ and $\tilde{\Delta}$ and hence also for any points in these triangles.

Now define a comparison triangle $\bar{\Delta} = \bar{\Delta}(\bar{x}, \bar{y}, \bar{z}) \subseteq \mathbb{S}^n$ of $\tilde{\Delta} \subseteq \mathbf{L}$ and let $a, b \in \Delta$ with embedded points $\tilde{a}, \tilde{b} \in \tilde{\Delta} \subseteq \mathbf{L}$ and comparison points $\bar{a}, \bar{b} \in \bar{\Delta} \subseteq \mathbb{S}^n$. Since $\mathbf{L}$ is CAT(1), $d_1(\bar{a}, \bar{b}) \geq d_{\mathbf{L}}(\tilde{a}, \tilde{b}) = d_{\mathrm{Lk}}(a, b)$. This holds for all $a, b \in \mathrm{Lk}(v, \mathbf{L})$, hence the link is CAT(1). □

Lemma 5.20. *Let $\mathbf{L}$ be an all-right spherical complex with finitely many faces. If $\mathbf{L}$ is not* CAT(1)*, then exists a geodesic loop of length $< 2\pi$ in $\mathbf{L}$.*

Proof. Consider $(\mathbf{L}, d)$ a non-CAT(1) all-right spherical complex with finitely many faces. Then there is a geodesic triangle $\Delta = \Delta(p, q, r) \subseteq \mathbf{L}$ of perimeter $P_\Delta < 2\pi$ and $x_1, y_1 \in \Delta$ such that for the comparison triangle $\bar{\Delta} \subseteq \mathbb{S}^n$ and comparison points $\bar{x}_1, \bar{y}_1 \in \bar{\Delta}$: $d(x_1, y_1) > d_1(\bar{x}_1, \bar{y}_1)$. By construction of the metric exists a geodesic c_1 joining x_1 and y_1 with $l(c_1) = d(x_1, y_1)$. Without loss of generality, $x_1, y_1 \neq p$ and consider the geodesic triangle Δ_1 build from the geodesic segments c_1, $[y_1, p]$ and $[p, x_1]$. It is non-degenerate and of perimeter $< 2\pi$ since it is inscribed in Δ. By construction, Δ_1 does not fulfill the CAT(1) inequality. Let x_2, y_2 the points that contradict the CAT(1) property (i.e. the analogues to x, y in Δ), then the procedure used to construct Δ_1 can be repeated to find a geodesic triangle Δ_2. Reiterating the procedure further times yields a minimal and non-degenerate triangle Δ_n. Define r to be less or equal to half the perimeter of this triangle, i.e. $P_{\Delta_n} \geq 2r$. Then consider $z, \tilde{z} \in \Delta_n$ such that $d(x_n, z) + d(x_n, \tilde{z}) = r$. By the triangle inequality, $d(z, \tilde{z}) \leq r$. If this inequality was strict, $(x, z, \tilde{z})$ would be the vertices of a triangle Δ_{n+1} of perimeter $P_{\Delta_{n+1}} = d(x_n, z) + d(x_n, \tilde{z}) + d(z, \tilde{z}) < r + r \leq P_{\Delta_n}$. This contradicts the minimality of Δ_n, thus $d(z, \tilde{z}) = r$ must hold and hence Δ_n is isometric to a circle. Since it is inscribed in Δ, $P_{\Delta_n} \leq P_\Delta < 2\pi$ and hence Δ_n is the proposed geodesic loop. □

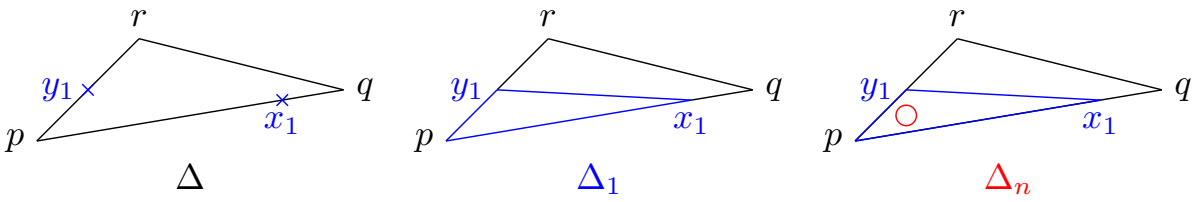

Figure 36: Setting of the proof of Lemma 5.20.

Lemma 5.21. *Consider a finite dimensional all-right spherical complex* $\mathbf{L}$*. If* $\mathbf{L}$ *is* CAT(1)*, then it is a flag complex.*

Proof. Let $\mathbf{L}$ be a finite dimensional all-right spherical complex. It suffices to show that for all $n \in \mathbb{N}$, $\mathbf{L}$ does not contain any empty skeletons (i.e. skeletons that are no simplices) of dimension n. Proof by induction:
$\underline{n = 1}$ is trivial since 1-skeletons contain two vertices only and are thus 1-simplices by construction.
$\underline{n = 2}$ Consider a 2-skeleton $\{x, y, z\}$ which gives a geodesic triangle $\Delta = \Delta(x, y, z)$. Assume $\{x, y, z\}$ is not a simplex. Then for m the midpoint of the geodesic segment $[x, y]$, $d_{\mathbf{L}}(m, z) = d_{\mathbf{L}}(m, y) + d_{\mathbf{L}}(y, z) = \frac{\pi}{2} + \pi = \frac{3\pi}{4}$. On the other hand, for $\bar{m}, \bar{z}$ the comparison points of m, z in $\mathbb{S}^2$, $d_1(\bar{m}, \bar{z}) = \frac{\pi}{2} < \frac{3\pi}{4} = d_{\mathbf{L}}(m, z)$ which contradicts the CAT(1) inequality.

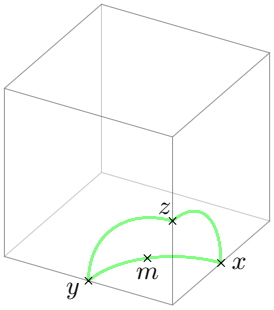

Figure 37: Setting in the proof of Lemma 5.21 for $n = 2$.

$\underline{n \to n + 1}$ Let $\{v_0, ..., v_{n+1}\}$ be an $(n+1)$-skeleton S. Fix one of its vertices v_i and consider its link $\mathrm{Lk}(v_i, \mathbf{L})$. It is a n-dimensional all-right spherical complex and by Lemma 5.19 it is CAT(1). Thus, by assertion, $\mathrm{Lk}(v_i, \mathbf{L})$ is flag. The intersection $S \cap \mathrm{Lk}(v_i, \mathbf{L})$ gives an n-skeleton in $\mathrm{Lk}(v_i, \mathbf{L})$ which is thus an n-simplex. Since this is true for all $v_i, i = 0, ..., n+1$, S is in fact an $(n + 1)$-simplex. □

Lemma 5.22. *Let* $\mathbf{L}$ *be a finite dimensional all-right spherical flag complex. Then it is* CAT(1)*.*

Proof. Consider $\mathbf{L}$ a finite dimensional all-right spherical flag complex. By Lemma 5.20, if all geodesic loops in $\mathbf{L}$ are of length greater or equal 2π, then $\mathbf{L}$ is CAT(1). Thus it suffices to proof that for all $n \in \mathbb{N}$, if $\mathbf{L}$ is of dimension n, it does not contain any geodesic loop of length less than 2π.
$\underline{n = 1}$ For simplicity, consider this case first. Here, all non-trivial simplices are of dimension 1, i.e. edges, and have length $\frac{\pi}{2}$. To build a geodesic loop, at least three of them have to be connected. The condition of the loop to have length less than 2π implies that is given by exactly three connected edges, e.g. as in Fig. 33. This is a 2-skeleton which is not a simplex (since $n = 1$) and thus contradicts the assumption that $\mathbf{L}$ is flag.

$\underline{n > 1}$ Let c be the image of a geodesic loop and v a vertex in $\mathbf{L}$, such that $c \cap B(v, \frac{\pi}{2}) \neq \emptyset$. Define $V_c = \{u \in V_\mathbf{L} \mid B(u, \frac{\pi}{2}) \cap c \neq \emptyset\}$ where $V_\mathbf{L}$ is the set of vertices of $\mathbf{L}$. Since all-right spherical shapes are parts of spheres, the geometry of a sphere implies that geodesic loops can not be contained in a single shape. In particular, c cannot lie in a single simplex and thus $V_c \setminus \{v\} \neq \emptyset$. Now assume $l(c) < 2\pi$, which implies $B(u, \frac{\pi}{2}) \cap B(w, \frac{\pi}{2}) \neq \emptyset$ for all $u, w \in V_c$, hence the elements of V_c are pairwise connected by edges. This means that V_c is a skeleton. Since $\mathbf{L}$ is flag, it is a simplex and by construction c is contained in this simplex. This contradicts the fact that a geodesic can not be contained in a single simplex. □

The combination of Lemma 5.21 and Lemma 5.22 gives the first characterization of CAT(1) needed to prove Theorem 5.17. A more general version of the second one was proven by [BH99] and [Gd90], but in this thesis we want to focus on the result for CAT(0) cube complexes and thus prove Theorem 5.25 only. To this end, we present a simplified proof based on the following preliminary lemma.

Lemma 5.23. *Consider a cubical complex $(\mathbf{K}, d_\mathbf{K})$ and a vertex $v \in \mathbf{K}$ with link complex $(\mathrm{Lk}(v, \mathbf{K}), d_{\mathrm{Lk}})$. For $a, b \in \mathrm{Lk}(v, \mathbf{K})$ consider the embedding $ta, tb \in \mathbf{K}$ for some $t \in (0, 1)$. Then, the Alexandrov angle $\alpha_v(a, b)$ in the geodesic triangle $\Delta = \Delta(v, ta, tb) \subseteq \mathbf{K}$ is given by $\alpha_v(a, b) = \min\{d_{\mathrm{Lk}}(a, b), \pi\}$ and is independent of t.*

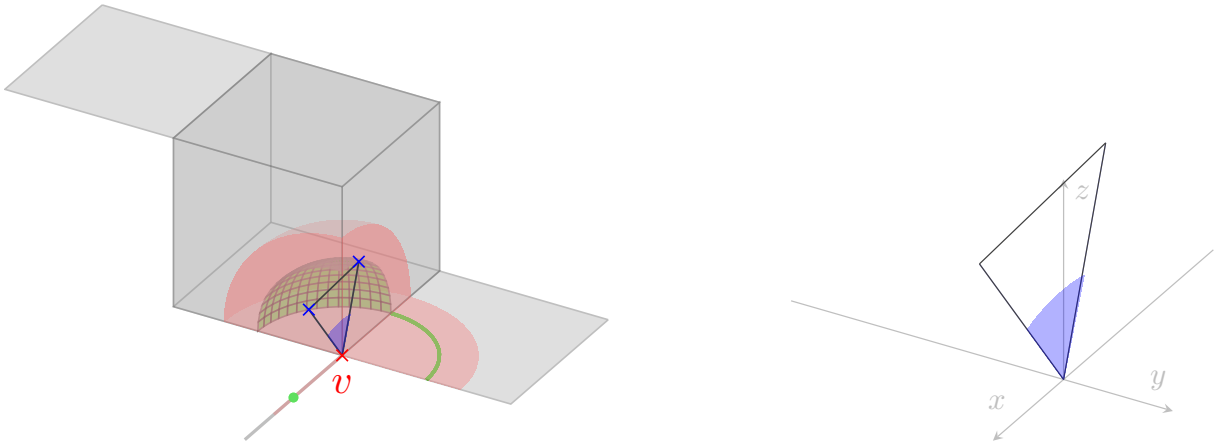

Figure 38: The metric of the link (green) can be related to the (blue) Alexandrov angle at the vertex v of the geodesic triangle (grey). The original triangle in the cube complex is displayed on the left, its comparison triangle on the right.

Proof. Let $(\mathbf{K}, d_\mathbf{K})$, $v \in \mathbf{K}$ and $(\mathrm{Lk}(v, \mathbf{K}), d_{\mathrm{Lk}})$ as in the lemma. Any $a, b \in \mathrm{Lk}(v, \mathbf{K})$ can be embedded into $\mathbf{K}$ as $ta, tb \in \mathbf{K}, t \in (0, 1)$ (Remark 5.14). For the geodesic triangle $\Delta = \Delta(v, ta, tb) \subseteq \mathbf{K}$, the Alexandrov angle α_v is independent of t by construction from the limit (Definition 2.14).

If $d_{\mathrm{Lk}}(a, b) \leq \pi$, the shortest path between $ta, tb \in \mathbf{K}$ (which is thus the geodesic segment $[ta, tb]$) lies within the embedding of the link $\mathrm{Lk}(v, \mathbf{K})$ into $\mathbf{K}$. The resulting

geodesic triangle $\Delta(v, ta, tb)$ has an Alexandrov angle of $\alpha_v(a, b)$ at v by construction, and since the embedding implies that the angle enclosed by $[v, ta]$ and $[v, tb]$ is $d_{\mathrm{Lk}}(a, b)$, one obtains $d_{\mathrm{Lk}}(a, b) = \alpha_v(a, b)$.

If $d_{\mathrm{Lk}}(a, b) > \pi$ exists a geodesic segment $[ta, tb] \subseteq \mathbf{K}$ that crosses the vertex v and is shorter than the path between ta, tb that lies in the embedding of $\mathrm{Lk}(v, \mathbf{K})$. Since $[ta, tb]$ is part of $\Delta(v, ta, tb)$ and crosses v, the Alexandrov angle at v is $\alpha_v(a, b) = \pi$ in this case. □

Definition 5.24. *Let* $\mathbf{K}$ *be a cube complex. If for all* v *vertices of* $\mathbf{K}$ *the link complex* $\mathrm{Lk}(v, \mathbf{K})$ *is* CAT(1)*,* $\mathbf{K}$ *is said to satisfy the* link condition*.*

Theorem 5.25. *Consider a finite dimensional cube complex* $\mathbf{K}$*. It is locally* CAT(0) *if and only if* $\mathbf{K}$ *satisfies the link condition.*

Proof. Let $\mathbf{K}$ be a finite dimensional cube complex. It is locally CAT(0) if and only if for every $x \in \mathbf{K}$ exists an $\epsilon_x > 0$ such that $B(x, \epsilon_x)$ is CAT(0).

For the implication "⇒" consider v a vertex in $\mathbf{K}$ and show that $\mathrm{Lk}(v, \mathbf{K})$ is CAT(1). Since $\mathbf{K}$ is locally CAT(0), there exists ϵ_v such that $B(v, \epsilon_v)$ is CAT(0). Let $\Delta \subseteq \mathrm{Lk}(v, \mathbf{K})$ be a triangle in $\mathrm{Lk}(v, \mathbf{K})$ with perimeter $P_\Delta < 2\pi$ and $a, b \in \Delta$. Then identify $a, b \in \mathrm{Lk}(v, \mathbf{K})$ with the corresponding directions in $\mathbf{K}$ and consider t such that $ta, tb \in B(v, \epsilon_v)$. Define $\tilde{\Delta} = \tilde{\Delta}(v, ta, tb)$ a geodesic triangle in $\mathbf{K}$ with comparison triangle $\bar{\Delta} = \bar{\Delta}(\bar{v}, \bar{ta}, \bar{tb}) \subseteq M_0^n = \mathbb{R}^n$. Since $B(v, \epsilon_v)$ is CAT(0), Theorem 2.16 implies $\alpha_v(a, b) = \alpha_v(ta, tb) \leq \gamma_{\bar{v}}$ for the Alexandrov angle α_v in $\mathbf{K}$. Here, $\gamma_{\bar{v}}$ is the comparison angle in $\bar{\Delta} \subseteq \mathbb{R}^n$ at the angle $\bar{v}$. This angle is the metric $d_1(\bar{a}, \bar{b})$ in the CAT(1) model space $M_1^n = \mathbb{S}^n$. On the other hand, $P_\Delta < 2\pi$ implies $P_{\hat{\Delta}} < 2\pi$ for the sub-triangle $\hat{\Delta} = \hat{\Delta}(a, b, p)$ with p a vertex of Δ. This together with the triangle inequality $d_{\mathrm{Lk}}(a, b) \leq d_{\mathrm{Lk}}(a, p) + d_{\mathrm{Lk}}(p, b)$ results in $d_{\mathrm{Lk}}(a, b) < \pi$. Hence, the Alexandrov angle α_v is equal to the metric in the link complex (Lemma 5.23) and $d_{\mathrm{Lk}}(a, b) = \alpha_v(a, b) \leq \gamma_{\bar{v}} = d_1(a, b)$.

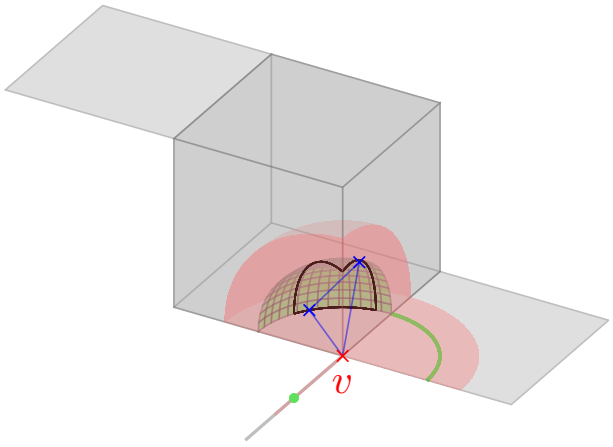

Figure 39: Setup for the "⇒"-part of Theorem 5.25, similar to Fig. 38. The triangle in the link, Δ, is given in black, the one in the cube complex, $\tilde{\Delta}$, in blue.

For "⇐", let w be a vertex in $\mathbf{K}$ and show the existence of $\epsilon_w > \frac{1}{2}$ such that $B(w, \epsilon_w) \subseteq \mathbf{K}$ is CAT(0). Given this for all vertices $w \in \mathbf{K}$, $\{B(w, \epsilon_w) \mid w \in \mathbf{K}\}$ cover $\mathbf{K}$. Thus, for every $x \in \mathbf{K}$ exists a vertex w and a number $\epsilon_x > 0$ such that $B(x, \epsilon_x) \subseteq B(w, \epsilon_w)$ and since $B(w, \epsilon_w)$ is CAT(0) so is $B(x, \epsilon_x)$.

For the remaining part of the proof, choose $w \in \mathbf{K}$ and $\epsilon_w > \frac{1}{2}$. Let $\Delta \subseteq B(w, \epsilon_w)$ a geodesic triangle and $p, q \in \Delta$. Consider the following cases:

(i) Let $w \notin [p, q]$. In this case, p and q can be written as $p = ta$ and $q = sb$ for some $a, b \in \mathrm{Lk}(w, \mathbf{K})$ and $t, s > 0$. Then $\alpha_w(a, b) \leq \pi$ and hence $d_{\mathrm{Lk}}(a, b) = \alpha_w(a, b)$ (Lemma 5.23). In this regime, the Cosine is monotonically descreasing. The link being CAT(1) implies $\alpha_w(a, b) = d_{\mathrm{Lk}}(a, b) \leq d_1(a, b) = \gamma_{\bar{w}}$. The latter is the angle in the comparison triangle in M_1^n. This can be embedded into the model space M_0^n of the cube complex such that $\gamma_{\bar{v}}$ is the angle at $\bar{v}$ in the comparison triangle $\bar{\Delta}$. Thus,

$$d^2_{\mathbf{K}}(p, q) = d^2_{\mathbf{K}}(ta, sb) = t^2 + s^2 - 2ts\cos(\alpha_w(a, b)) \tag{22}$$
$$\leq t^2 + s^2 - 2ts\cos(\gamma_{\bar{w}}) \tag{23}$$
$$= d_0^2(\bar{p}, \bar{q}) \tag{24}$$

by the law of cosines (Lemma 2.5) and with $\bar{p}, \bar{q}$ being the comparison points of p, q.

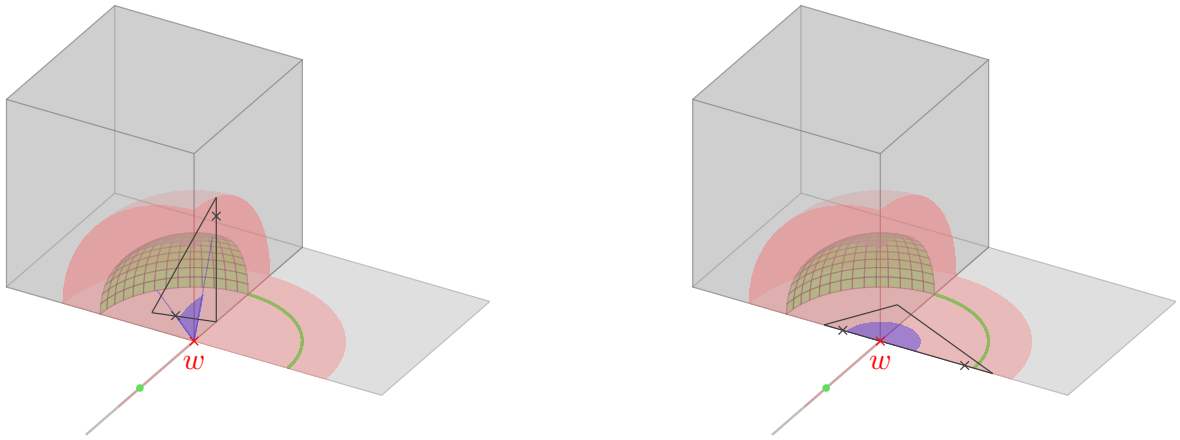

(i) (ii)

Figure 40: Setting for the proof of the "⇐"-implication of Theorem 5.25, part (i) on the left and part (ii) on the right, similar to Fig. 38. The geodesic triangles in the cube complex are given in grey. The distance of the two points marked on their circumference can be related to the blue angle, which gives the metric of the link.

(ii) Let $w \in [p, q]$. For $p = ta$ and $q = sb$ with $t, s > 0$ and $a, b \in \mathrm{Lk}(w, \mathbf{K})$ one obtains

$$d_{\mathbf{K}}(p, q) = d_{\mathbf{K}}(p, w) + d_{\mathbf{K}}(w, q) = t + s = d_0(p, q) \tag{25}$$

in this case.

Thus, the CAT(0) inequality holds for all cases. This concludes the proof. □

Proof of of Theorem 5.17. Consider $\mathbf{K}$ a finite dimensional cube complex. By Definition 2.12, it has curvature ≤ 0 if and only if it is locally CAT(0). This is equivalent to $\mathbf{K}$ satisfying the link condition, as stated in Theorem 5.25. Lemma 5.22 for the if-part and Lemma 5.21 for the only-if-part yield the equivalence of this condition to the property that for every vertex v of $\mathbf{K}$ the link complex $\mathrm{Lk}(v, \mathbf{K})$ flag. □

6 CAT(0) chart complexes

Throughout this chapter, consider $\mathcal{Q}$ a quiver and $\mathfrak{T}$ a set of consistent sub-atlases on $\mathcal{Q}$. Its elements are defined as given in Remark 4.19.

Definition 6.1. *For a consistent sub-atlas $T \in \mathfrak{T}$ with dimension n, define the* faces *of T to be the subsets of T. All transitions between two charts C, C' in such a face are also possible between charts in T since $C, C' \in T$. This implies that the face must be consistent and of dimension $\leq n$. Hence, the faces of T are consistent sub-atlases of smaller dimension than T.*

Definition 6.2. *Let $T, \tilde{T}$ be two consistent sub-atlases, $O \subseteq T$ a face of T and $\tilde{O} \subseteq \tilde{T}$ a face of $\tilde{T}$. Then define a* gluing *of T and $\tilde{T}$ to be a mapping $\phi : O \to \tilde{O}$ such that for all charts $C \in O \cap \tilde{O}$ holds: $\mathtt{a} \in \phi(C) \Leftrightarrow \mathtt{a} \in C$, i.e. $\phi(C)$ and C are the same up to ordering of cardinals.*

Definition 6.3. *Consider $\mathfrak{T}$ a set of consistent sub-atlases on $\mathcal{Q}$. With the definition of gluing from Definition 6.2, one can construct a* chart complex $\mathbf{K}_{\mathfrak{T}}$ *in the same way a as described in Definition 5.6.*

Remark 6.4. The vertices of the chart complex $\mathbf{K}_{\mathfrak{T}}$ are given by the vertices of the consistent sub-atlases factorized by the equivalence relation defined by the gluings. Since the vertices of the consistent sub-atlases are given by the 0-dimensional consistent sub-atlases, i.e. the charts (Remark 4.19), the set of vertices of the chart complex is $V_{\mathfrak{T}} = \{C \text{ unordered chart} \mid \exists T \in \mathfrak{T} \text{ with } C \in T\}$. With the definition of faces of a consistent sub-atlas from Definition 6.1, the set of faces of $\mathbf{K}_{\mathfrak{T}}$ is $F_{\mathfrak{T}} = \bigcup_{T \in \mathfrak{T}} \{O \subseteq T\}$, i.e. the union of the power sets of the consistent sub-atlases.

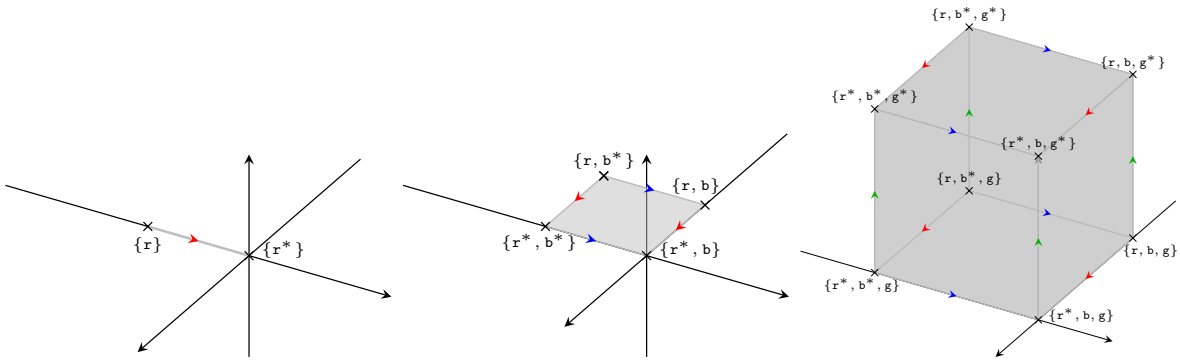

Figure 41: Examples of how a chart with $n = 1, 2, 3$ cardinals relates to an n-dimensional cube. In the language of consistent sub-atlases, a chart C gives a sub-atlas T_C that contains C and the charts obtained from C by inverting transitions (Remark 4.9). It is consistent by construction and its dimension is the number of cardinals present in the chart C, i.e. n in this example.

The examples in Fig. 41 suggest that any chart C defines a consistent sub-atlas T_C that can be visualized as a cube. This leads to the following conjecture:

Conjecture 6.5. *Any consistent sub-atlas $T \in \mathfrak{T}$ of dimension n corresponds to an n-cube (Definition 5.1). In this way, the chart complex $\mathbf{K}_{\mathfrak{T}}$ can be treated as a cube complex (Definition 5.6).*

As noted in Remark 5.14, the link complex at a certain vertex is given by the directions at that vertex. In the setting of chart complexes, the vertices are given by the charts and the shapes in which the directions must lie are the consistent sub-atlases. The directions are thus the directions from one chart to the other, i.e. the transitions.

Conjecture 6.6. *Consider a chart complex $\mathbf{K}_{\mathfrak{T}}$ and a vertex C of this chart complex, which by Remark 6.4 is a chart. Then the link at C is given by $\mathrm{Lk}(C, \mathbf{K}_{\mathfrak{T}}) = \{\rho_{C,\tilde{C}} \mid \exists T \in \mathfrak{T}$ with $C, \tilde{C} \in T\}$, where $\rho_{C,\tilde{C}}$ is a transition from C to $\tilde{C}$. In this sense, the link is the set of transitions from C to any other chart that lies in a consistent sub-atlas which contains C.*

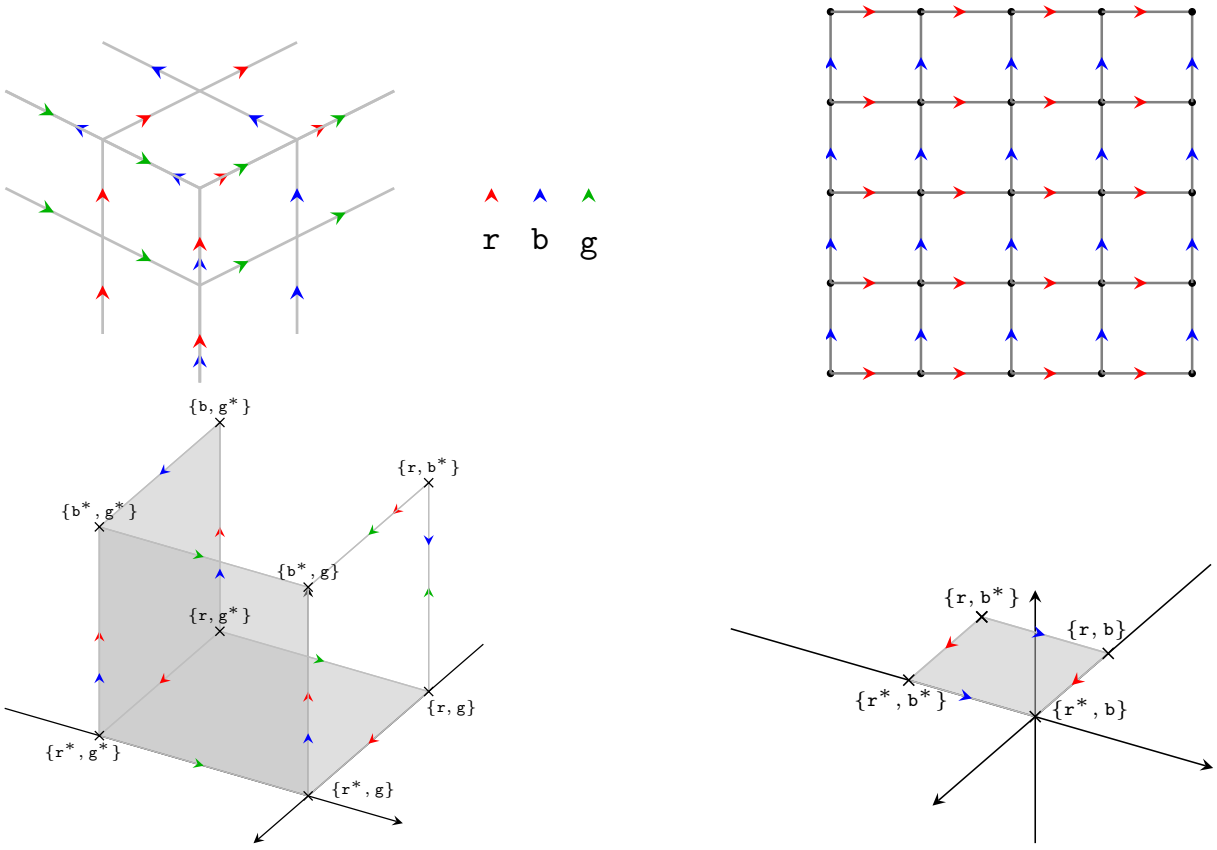

Figure 42: Examples for quivers with (left, denoted $\mathcal{W}$) and without (right, denoted $\mathcal{L}$) chart defects (above) and parts of their respective chart complexes $\mathbf{K}_{\mathcal{W}}$ and $\mathbf{K}_{\mathcal{L}}$ (below). The arrows in the chart complexes indicate the corresponding cardinal rewrites. The link $\mathrm{Lk}(\{\mathtt{r}^*, \mathtt{g}^*\}, \mathbf{K}_{\mathcal{W}})$ is not flag and $\mathcal{W}$ harbours a chart defect.

Lemma 6.7. *For a quiver $\mathcal{Q}$ consider a chart C such that the set $\{\rho_{C,\tilde{C}} \mid \exists T \in \mathfrak{T}$ with $C, \tilde{C} \in T\}$ has a subset L which satifies the following:*

(i) L does not contain inverting transitions (Remark 4.9).

(ii) In the union of chart rewrites $R = \bigcup_{\rho \in L} R_\rho$ exist rewrites with composition $\mathtt{a} \mapsto \mathtt{a}^*$ for some cardinal $\mathtt{a}$.

Then $\mathcal{Q}$ harbours a chart defect.

Proof. In this setting, L is a set of transitions from C to charts that have domains that overlap with the domain of C (by the definition of transitions). Hence, a cardinal transport between the charts can be defined. This cardinal transport is inconsistent according to Definition 4.16. Thus, the set of charts $\{\tilde{C} \mid \rho_{C,\tilde{C}} \in L\}$ cannot be combined to a consistent sub-atlas. This inconsistency gives the existence of a chart defect (Definition 4.17). □

By Conjecture 6.6, the assumptions for Lemma 6.7 are given if there exists a chart C with its link $\mathrm{Lk}(C, \mathbf{K}_\mathfrak{T})$ not being flag. Thus, this implies that $\mathcal{Q}$ harbours a chart defect.

Conversely, if $\mathcal{Q}$ has a chart defect, i.e. the atlas of $\mathcal{Q}$ is inconsistent, let T be the sub-atlas containing the charts that are part of this inconsistency. By considering the inverting transitions of these charts in the way the vertical 2-cubes of $\mathbf{K}_\mathcal{W}$ in Fig. 42 are constructed, T gives faces in the chart complex that surround the inconsistency. Thus, the corresponding links contain skeletons that are no simplices, i.e. are not flag. This suggests the following equivalence.

Conjecture 6.8. *A quiver $\mathcal{Q}$ with $\mathfrak{T}$ the set of all of its consistent sub-atlases does not harbour any chart defect if and only if for all of the charts C of $\mathcal{Q}$, i.e. the vertices of its chart complex $K_\mathfrak{T}$, the link $\mathrm{Lk}(C, \mathbf{K}_\mathfrak{T})$ is flag.*

Furthermore, by Theorem 5.17 the condition that the links of all charts, i.e. vertices of the chart complex $\mathbf{K}_\mathfrak{T}$, are flag holds if and only if $\mathbf{K}_\mathfrak{T}$ is CAT(0).

Conjecture 6.9. *The chart complex $\mathbf{K}_\mathfrak{T}$ of a quiver $\mathcal{Q}$ with $\mathfrak{T}$ the set of all of its consistent sub-atlases is* CAT(0) *if and only if no chart defect is present in $\mathcal{Q}$.*

This, together with Lemma 4.20 stating that the condition of $\mathcal{D}$ being CAT(0) is equivalent to not having any chart defect gives an interesting correspondence between a quiver and its chart complex.

Conjecture 6.10. *Let $\mathcal{D}$ be a square lattice with defects. Then $\mathcal{D}$ is* CAT(0) *if and only if its chart complex is* CAT(0).

7 Conclusion and outlook

The aim of this thesis was to provide a simpler proof of Gromov's link condition and to investigate the application to discrete cases. To achieve this, I avoided the concepts of cones but focused on special cases for certain values of κ and the relation between the metrics of the cube complex and its link.

Furthermore, I found that the property of a quiver to be CAT(0) is related to the non-existence of positive vertex defects, which in turn can be connected to chart defects and the chart complex of a quiver. A summary of this is given in Fig. 43.

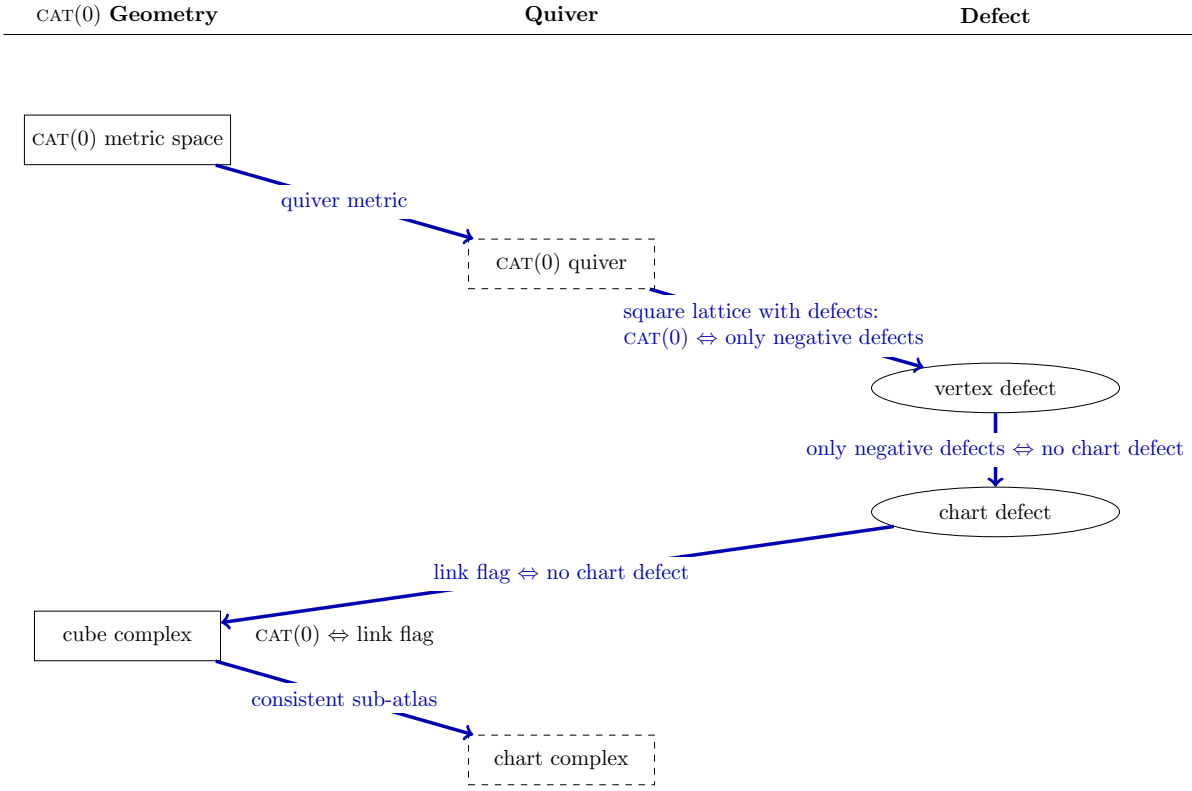

Figure 43: Relations of the concepts in this thesis.

Interestingly, negative vertex defects do not have any effect on the quiver's geometry in terms of the CAT(0) property. Finding a similar property that is related to this kind of defect could reveal further insightful results.

Additionally, it would be exciting to relate the concept of quiver calculus, which is currently being constructed and relates to Riemannian geometry on manifolds [Sei21], to the notion of curvature discussed here. As proven in Section 2.3, this is possible for manifolds and transferring the concepts needed for the proof to the discrete setting could yield further insights.

Concludingly, the field of CAT(κ) geometry is a very rich one when it comes to general metric spaces such as quivers and the combination with the discrete setting enables new findings.

Acknowledgements

I would like to thank my supervisor JProf. Dr. Beatrice Pozzetti for her guidance and support throughout the development of this thesis. Thank you for answering to all my questions and pointing me towards the right directions to learn more. This thesis would not have been possible either without the help of Taliesin Beynon, my mentor at the Wolfram Summer School 2021 and beyond. Thank you for introducing me to quiver geometry and for several insightful quiver-related meetings. I also want to thank the whole team of the Wolfram Summer School for the opportunity to participate and to gain more knowledge about quivers.

Furthermore, I am deeply thankful to my family and friends who supported me throughout my studies and the duration of this thesis. In particular, I thank Margarethe Hausmann, Frederik Kortkamp and Leonie Seifert for proofreading the thesis (and I apologize for not having mentioned any cat in a thesis about CAT(0) geometry).

References

[Ale51] A. D. Alexandrov. "Ein Satz über Dreiecke im metrischen Raum und einige Anwendungen". Russian. In: *Tr. Mat. Inst. Steklova* 38 (1951), pp. 5–23. ISSN: 0371-9685.

[Bey21] T. Beynon. *Quiver Geometry*. 2021. URL: `https://quivergeometry.net/`.

[BH99] M. R. Bridson and A. Haefliger. *Metric spaces of non-positive curvature*. 1st ed. Grundlehren der mathematischen Wissenschaften. Berlin, Germany: Springer, Oct. 1999.

[Car25] E. Cartan. *La géométrie des espaces de Riemann*. French. Gauthier-Villars, 1925. URL: `http://eudml.org/doc/192543`.

[DM99] M. Davis and G. Moussong. "Notes on nonpositively curved polyhedra". In: *Low dimensional topology*. Budapest: János Bolyai Math. Soc., 1999, pp. 11–94.

[Gd90] E. Ghys and P. de la Harpe, eds. *Sur les Groupes Hyperboliques d'après Mikhael Gromov*. Boston: Birkhäuser, 1990.

[Gro87] M. Gromov. "Hyperbolic Groups". In: *Essays in Group Theory*. New York: Springer, 1987, pp. 75–263.

[Mey89] W. Meyer. *Topogonov's Theorem and Applications*. Trieste: College on Differential Geometry, 1989.

[Sch19] P. Schwer. *Lecture notes on CAT(0) cube complexes*. 2019. arXiv: `1910.06815 [math.GR]`.

[Sei21] A. Seifert. *Lie algebras and curvature in discrete geometry*. 2021. URL: `https://community.wolfram.com/groups/-/m/t/2314740`.

List of Figures

Erklärung

Ich versichere, dass ich diese Arbeit selbstständig verfasst und keine anderen als die angegebenen Quellen und Hilfsmittel benutzt habe.

Heidelberg, den 7. Februar 2022,

Antonia Seifert